AD-A136 054 FRACTURE BEHAVIOR UNDER IMPACT(U) FRAUNHOFER-INST FUER 1/1
WERKSTOFFMECHANIK FREIBURG (GERMANY F R)
J F KALTHOFF ET AL. JAN 82 W-8/83 DAJA37-81-C-0013
UNCLASSIFIED F/G 20/11 NL

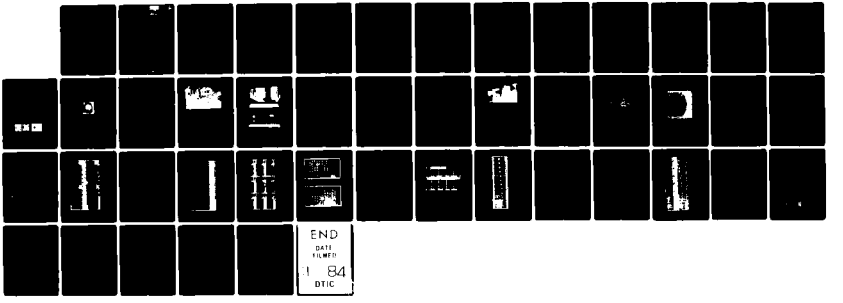

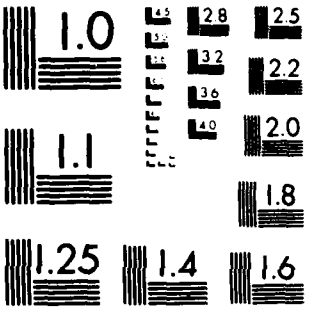

Fraunhofer-Gesellschaft

FRACTURE BEHAVIOR UNDER IMPACT

W 8/83

First Annual Report

by

J.F. Kalthoff and S. Winkler

Reporting Period Feb. 1981 - Jan. 1982

Fraunhofer-Institut
für Werkstoffmechanik

UNCLASSIFIED

SECURITY CLASSIFICATION OF THIS PAGE (When Data Entered)

R&D 3012-AN

REPORT DOCUMENTATION PAGE		READ INSTRUCTIONS BEFORE COMPLETING FORM
1. REPORT NUMBER	2. GOVT ACCESSION NO. AD-A136 054	3. RECIPIENT'S CATALOG NUMBER
4. TITLE (and Subtitle) Fracture Behavior under Impact		5. TYPE OF REPORT & PERIOD COVERED First Annual Report FEB 81 - JAN 82
		6. PERFORMING ORG. REPORT NUMBER
7. AUTHOR(s) J.F. Kalthoff and S. Winkler		8. CONTRACT OR GRANT NUMBER(s) DAJA37-81-C-0013
9. PERFORMING ORGANIZATION NAME AND ADDRESS Fraunhofer-Institut für Werkstoffmechanik Wöhferstr. 11,7800 Freiburg/Brsg. West Germany		10. PROGRAM ELEMENT, PROJECT, TASK AREA & WORK UNIT NUMBERS 6.11.02A IT161102BH57-06
11. CONTROLLING OFFICE NAME AND ADDRESS USARDSG-UK		12. REPORT DATE FEB 81 - JAN 82
		13. NUMBER OF PAGES 41
14. MONITORING AGENCY NAME & ADDRESS(if different from Controlling Office)		15. SECURITY CLASS. (of this report) Unclassified
		15a. DECLASSIFICATION/DOWNGRADING SCHEDULE

16. DISTRIBUTION STATEMENT (of this Report)

Approved for public release; distribution unlimited.

17. DISTRIBUTION STATEMENT (of the abstract entered in Block 20, if different from Report)

18. SUPPLEMENTARY NOTES

19. KEY WORDS (Continue on reverse side if necessary and identify by block number)

dynamic fracture, impact loading, crack instability, dynamic stress intensity factor, impact fracture toughness, stress optical techniques shadow optical method of caustics.

20. ABSTRACT (Continue on reverse side if necessary and identify by block number) The physical behavior of cracks under impact loading is investigated. Single edge cracks or arrays of multiple cracks in rectangular specimens are considered. the specimens are loaded by time dependent tensile stress pulses moving perpendicular to the crack direction. The specimens are directly loaded by an impinging projectile or by a base plate which is accelerated by a projectile. The specimens are made from a transparent model material or a high strength steel. The initial crack lengths and impact velocities are varied throughout the experiments. Utilizing

DD FORM 1 JAN 73 1473 EDITION OF 1 NOV 65 IS OBSOLETE

UNCLASSIFIED

SECURITY CLASSIFICATION OF THIS PAGE (When Data Entered)

20) the shadow optical method of caustics in combination with high speed photography, the dynamic stress intensity factors at the tip of the crack are measured as functions of time during the impact event. The critical value of the dynamic stress intensity factor at onset of rapid crack propagation, i.e. the dynamic fracture toughness $K_{Id}m$ is determined and discussed with regard to the time t_f at which the crack becomes unstable. The results are compared to corresponding static fracture toughness data.

Within the first year of the three year's research project the experimental set-up has been built up. The IWM-gas gun has been modified for this purpose. A Cranz-Schardin high speed camera operated in a shadow optical arrangement has been aligned to the gas gun. A holding fixture has been designed and built to load the specimens under direct and base plate loading conditions, in particular the load pulse history in the specimen has been studied. Several series of experiments with precracked specimens have been performed to specify the parameters for the following main investigations. The work has been progressing according to the proposed schedule.

AD

FRACTURE BEHAVIOR UNDER IMPACT

W 8/83

First Annual Report

by

J.F. Kalthoff and S. Winkler

Reporting Period Feb. 1981 - Jan. 1982

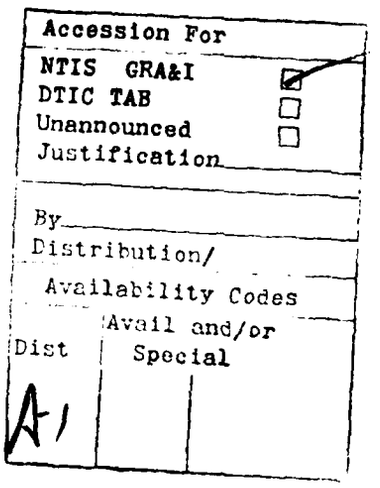

United States Army

EUROPEAN RESEARCH OFFICE OF THE U.S. Army

London England

CONTRACT NUMBER DAJA 37-81-C-0013

Fraunhofer-Institut für Werkstoffmechanik
Wöhlerstr. 11, 7800 Freiburg/Brsg., West-Germany

ABSTRACT

The physical behavior of cracks under impact loading is investigated. Single edge cracks or arrays of multiple cracks in rectangular specimens are considered. The specimens are loaded by time dependent tensile stress pulses moving perpendicular to the crack direction. The specimens are directly loaded by an impinging projectile or by a base plate which is accelerated by a projectile. The specimens are made from a transparent model material or a high strength steel. The initial crack lengths and impact velocities are varied throughout the experiments. Utilizing the shadow optical method of caustics in combination with high speed photography, the dynamic stress intensity factors at the tip of the crack are measured as functions of time during the impact event. The critical value of the dynamic stress intensity factor at onset of rapid crack propagation, i.e. the dynamic fracture toughness K_{Id}, is determined and discussed with regard to the time t_f at which the crack becomes unstable. The results are compared to corresponding static fracture toughness data.

Within the first year of the three year's research project the experimental set-up has been built up. The IWM-gas gun has been modified for this purpose. A Cranz-Schardin high speed camera operated in a shadow optical arrangement has been aligned to the gas gun. A holding fixture has been designed and built to load the specimens under direct and base plate loading conditions, in particular the load pulse history in the specimen has been studied. Several series of experiments with precracked specimens have been performed to specify the parameters for the following main investigations. The work has been progressing according to the proposed schedule.

KEYWORDS: dynamic fracture, impact loading, crack instability, dynamic stress intensity factor, impact fracture toughness, stress optical techniques, shadow optical method of caustics

CONTENTS

1 INTRODUCTION

The failure behavior of structures which contain cracks or crack-like defects in general is very well understood. The concept of fracture mechanics provides a powerful tool for quantitative safety predictions:

- The stress intensity factor, K, is a measure of the severity or criticality of a crack. The main parameters which determine this mechanical property are the length of the crack and the load which is applied to the crack.

- The fracture toughness, K_{Ic}, i.e. the critical stress intensity factor for onset of rapid crack propagation, is a material property which describes the resistance of the material to crack extension.

For static or quasistatic loading conditions this concept has been successfully applied to many cases of practical importance:

- Formulas have been established to determine (exactly or at least approximately) the static stress intensity factor K_I^{stat} for almost any crack problem.

- Standardized test procedures have been developed to measure the static fracture toughness K_{Ic} for different materials.

- Design criteria have been formulated on the basis of these two properties, i.e. K^{stat} and K_{Ic}, which allow the assessment of the safety of a structure under the specific service conditions [1,2].

The fracture behavior of cracks subjected to dynamic loading is considerably less well understood. The reason for this situation is the fact that these problems are far more complicated. The stress intensification at the crack tip becomes a complicated function of time and consequently, the instability event is controlled by a rather complex process which cannot be described by simple means.

Thus, the most commonly used dynamic material strength value still is the Charpy energy, i.e. the energy to break a Charpy V-notch specimen in a pendulum type impact tester. This material property represents only a relative material characterisation which cannot be used for quantitative design purposes. Work is performed to develop a test procedure for measuring the dynamic fracture toughness value under impact loading, i.e. the impact fracture toughness K_{Id}. A currently proposed procedure for measuring this quantity in instrumented impact tests [3], however, is based on a simplyfied static evaluation procedure which determines the stress intensity factor from load values measured at the tup of the striking hammer via static stress intensity factor formulas. Fig. 1 compares these static stress intensity factors K^{stat} with the actual dynamics stress intensity factors at the crack tip, denoted K_I^{dyn} [4]. The differences are quite large, in particular at early times of the impact event. The differences have not vanished even after a

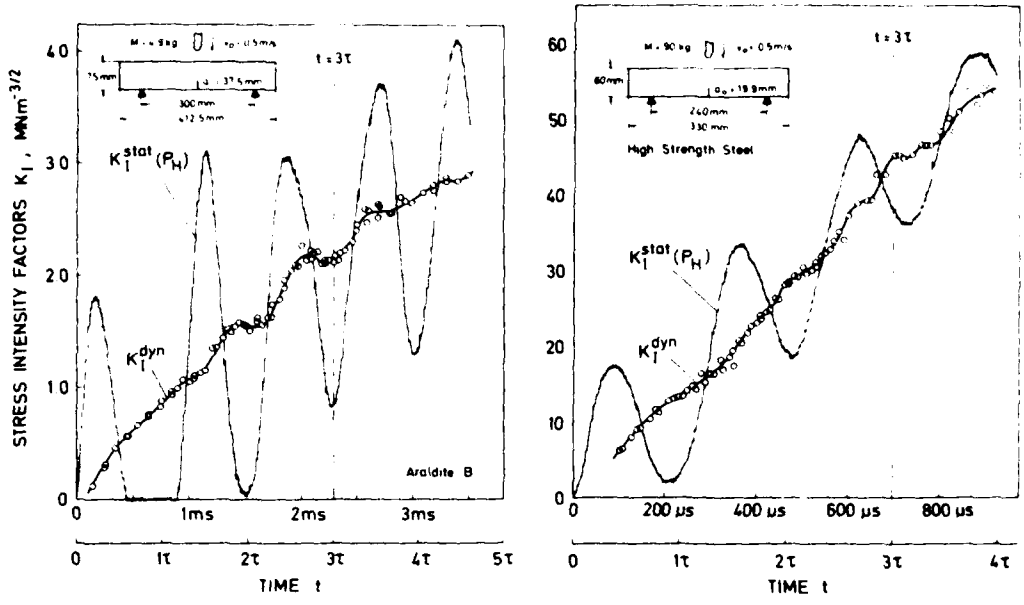

Fig. 1 Stress intensity factors for precracked bend specimens under drop weight loading

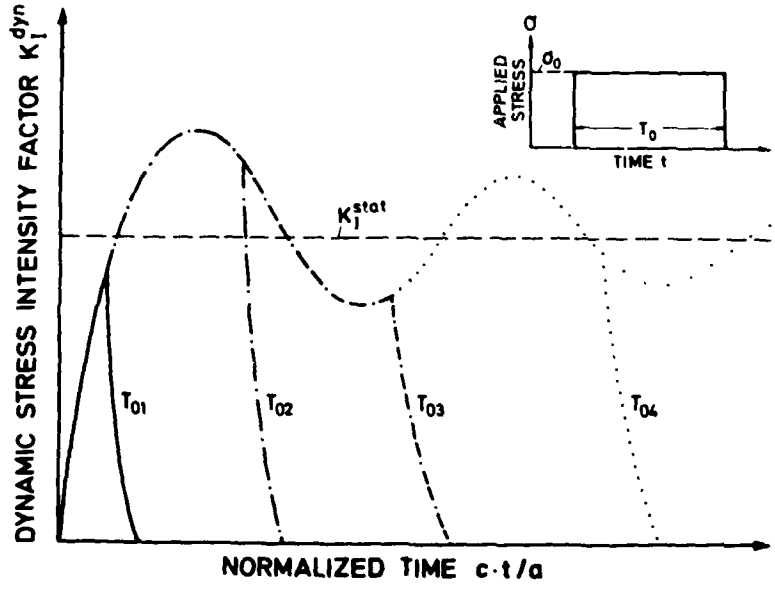

Fig. 2 Dynamic stress intensity factor for a crack under step function loads of durations $T_{01} < T_{02} < T_{03} < T_{04}$, schematically

time of 3τ, where τ is the period of the eigenoscillation of the specimen (see [3]). This procedure, therefore, is only applicable for very large times to fracture which, however, can only be obtained when the impact velocity is reduced to very low values. Depending on the test conditions the maximum tolerable impact velocity has to be as low as about 1 m/s [3].

Another example which demonstrates the complex behavior of dynamic stress intensifications is shown in Fig. 2. For a crack of length a under mode I step function load of duration T_o the dynamic stress intensity factor is plotted as a function of time (see [5-9]). The dimensionless time unit $(c_1 t)/a_o$ is used in this diagram, where c_1 is a wave velocity. K_I^{dyn} increases with time according to a $\sqrt{t}$ dependence, overshoots the equivalent static stress intensity factor K_I^{stat} up to 30%, and for larger times only approaches K_I^{stat} by an oscillation with a damped amplitude. The duration T_o of the pulse controls the physically valid time interval (see Fig. 2). Because of the complicated $K_I^{dyn}(t)$ behavior, especially for short pulse durations, conclusions on the effective stress intensity factor for the impact event can hardly be made. The maximum value of the $K_I^{dyn}(t)$ curve cannot control the actual instability event, because this value is only active for a very short time and does not allow the crack to make large jumps. On the basis of energy and momentum considerations, Steverding and Lehningk [10-13] developed a dynamic fracture criterion which correlates the critical crack lengths with the applied pulse durations. A similar but more general criterion was developed later by Kalthoff and Shockey [14-17] denoted as minimum time fracture criterion.

These influences of time effects on the stress condition can have severe influences on procedures for measuring dynamic fracture toughness values. Impact fracture toughness data have been measured at different loading rates. Depending on the strain rate sensitivity of the material, K_{Id} decreases more or less strongly with increasing loading rate $\dot{\sigma}_o$, as is indicated in Fig. 3. Most of the dynamic fracture toughness data have been obtained in the lower impact velocity range with Charpy - and drop weight tests. An overview of the results obtained and the problems encountered in measuring these quantities is given in the papers of Turner, Venzi, Shoemaker, Rolfe, Loss, Ireland, Wullert, and others [18-22]. Data at higher loading rates have been measured for example by Costin, Duffy, Freund, and Server [23-24] with Hopkinson bar experiments, by Shockey, Curran, Homma and Kalthoff [17,25,26] with flyer plate impact experiments, and by Ravi Chandar and Knauss [27] using electromagnetic loading techniques. In their papers Eftis and Krafft [28] and Shockey and Curran [25] discuss the interesting question whether a minimum value of K_{Id} exists, which cannot be reduced even if the loading rate would be increased further (see Fig. 3).

The difficulty in all the measuring procedures consists of establishing a relation between quantities measured externally at the test machine and the actual stress intensity factor existing at the tip of the crack in the specimen. Different approaches are used: Simplyfied static ana-

lyses (e.g. with Charpy tests [3]), theoretical analyses which sometimes are based on nonrealistic assumptions (e.g. infinite boundaries or step function loads [5-9]), or numerical analyses which necessarily are very complicated. In this project the problem of deriving the stress intensity factor from secondary quantities measured in an experiment shall be avoided by measuring the actual dynamic stress intensity factor directly at the crack tip by a special optical technique developed at the Fraunhofer-Institut für Werkstoffmechanik, i.e. the shadow optical method of caustics.

The investigations are aimed to generate basic information on the failure behavior of precracked specimens with finite boundaries subjected to dynamic tensile stresses. The results shall be of special importance for the development of improved impact fracture toughness tests and the assessment of the load carrying capacity of structures under dynamic loading conditions in general.

2 GENERAL OUTLINE

2.1 Technical Objectives

The physical behavior of cracks under impact loading is investigated. Single edge cracks or arrays of multiple cracks in rectangular specimens are considered. The specimens are loaded by time dependent tensile stress pulses $p(t)$ moving perpendicular to the crack direction. The pulses are produced by impinging projectiles. The specimens are made from a transparent model material or a high strength steel. Utilizing the shadow optical method of caustics in combination with high speed photography, the dynamic stress intensity factors, K_I^{dyn}, at the tip of the crack are measured as functions of time during the impact event. The critical value of the dynamic stress intensity factor at onset of rapid crack propagation, i.e. the dynamic fracture toughness K_{Id}, is determined and compared to the corresponding static fracture toughness K_{Ic}. The results are discussed with regard to the times t_f at which the initial cracks become unstable.
Two kinds of impact experiments are envisaged in the research program:

A) Direct impact loading: The precracked specimen is directly impacted by the projectile. After passage of the compressive stress pulse through the specimen and reflection of the pulse at the free end of the specimen, the crack is loaded by tensile stresses (see schematic drawing - Fig. 4a).
B) Base plate loading: The precracked specimen is loaded in tension by a base plate which is accelerated by the impinging projectile (see schematic drawing - Fig. 4b).

The investigation of single edge cracks (as shown in the lower specimen of Fig. 4b) or arrays of multiple cracks (as shown e.g. in the upper specimen of Fig. 4b) is planned.

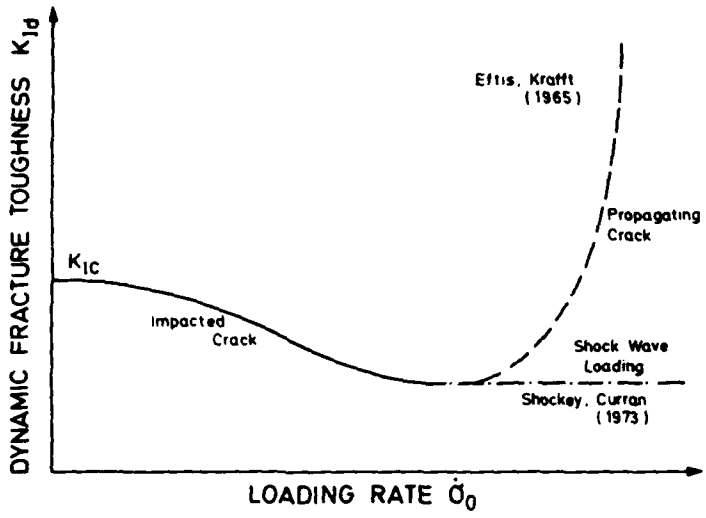

Fig. 3 Dynamic fracture toughness as a function of loading rate, (schematically)

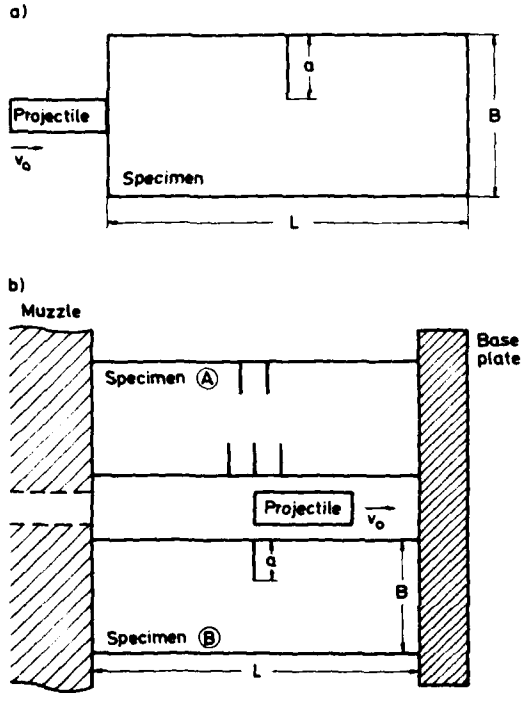

Fig. 4 Loading conditions, a) direct impact loading, b) base plate loading (schematically)

2.2 The Shadow Optical Method of Caustics

The method of caustics is an optical tool for measuring stress intensifications. The technique has been introduced by Manogg in 1964 [29,30]. Later on, Theocaris [31] further developed the method. The authors and their coworkers extended and applied Manoggs technique for investigating dynamic fracture phenomena [4, 32-38].

The physical principle of the method is illustrated in Fig. 5. A precracked specimen under load is illuminated by a parallel light beam. A cross-section through the specimen at the crack tip is shown in Fig. 5b for a transparent specimen, and in Fig. 5c for a non-transparent steel specimen. Due to the stress concentration the physical conditions at the crack tip are changed. For transparent specimens both the thickness of the specimen and the refractive index of the material are reduced. Thus, the area surrounding the crack tip acts as a divergent lens and the light rays are deflected outwards. As a consequence, on a screen (image plane) at a distance z_0 behind the specimen a shadow area is observed which is surrounded by a region of light concentration, the caustic (see Fig. 6). Fig. 5c shows the situation for a non-transparent steel specimen with a mirrored front surface. Due to the surface deformations light rays near the crack tip are reflected towards the center line. An extension of the reflected light rays onto a virtual image plane at the distance z_0 behind the specimen results in a light configuration which is similar to the one obtained in transmission. Consequently a similar caustic is obtained. The mode I shadow pattern was calculated by Manogg [30] from the linear elastic stress strain field around the crack tip. Fig. 6 compares theoretical results with experimentally observed caustics which were photographed in transmission and in reflection with different materials. The single caustic curve obtained for isotropic materials splits up into a double caustic for optically anisotropic materials.

The size of the shadow pattern is related to the stress intensification at the crack tip. The quantitative correlation between the diameter D of the caustic and the stress intensity factor K_I is given by the equation

$$K_I = M \cdot D^{5/2} \qquad (1)$$

where M is a known numerical factor which depends on the optical arrangement and the material utilized [32, 33].

A quantitative shadow-optical analysis is also available for cracks subjected to superimposed tensile (mode I) and shear (mode II) loading. With increasing ratio $\mu = K_{II}/K_I$ the caustic becomes asymmetrical (see Fig. 7a). Fig. 7b shows the theoretically calculated caustic in comparison to an experimentally observed shadow pattern for the case $\mu = 1$. From the minimum and maximum diameters D_{min} and D_{max} of the caustics (defined in Fig. 7b) the absolute values of the stress intensity factors K_I and K_{II} can be determined using the relation

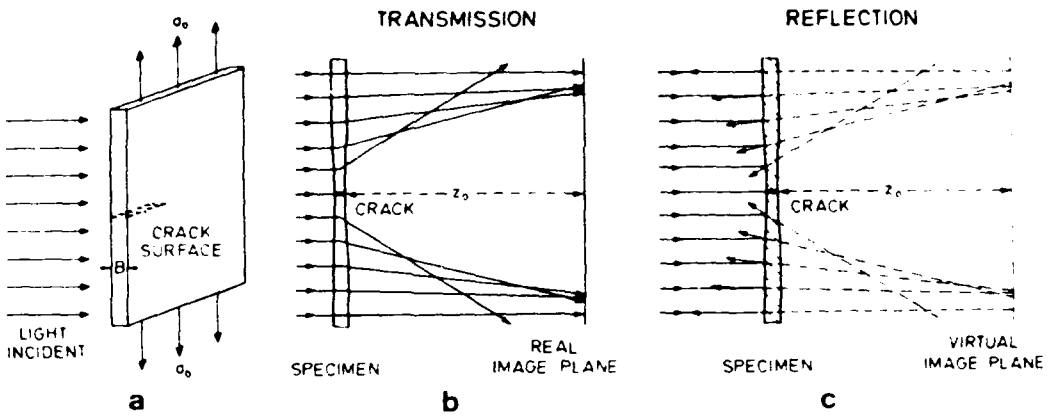

Fig. 5 Physical principles of the shadow optical method of caustics

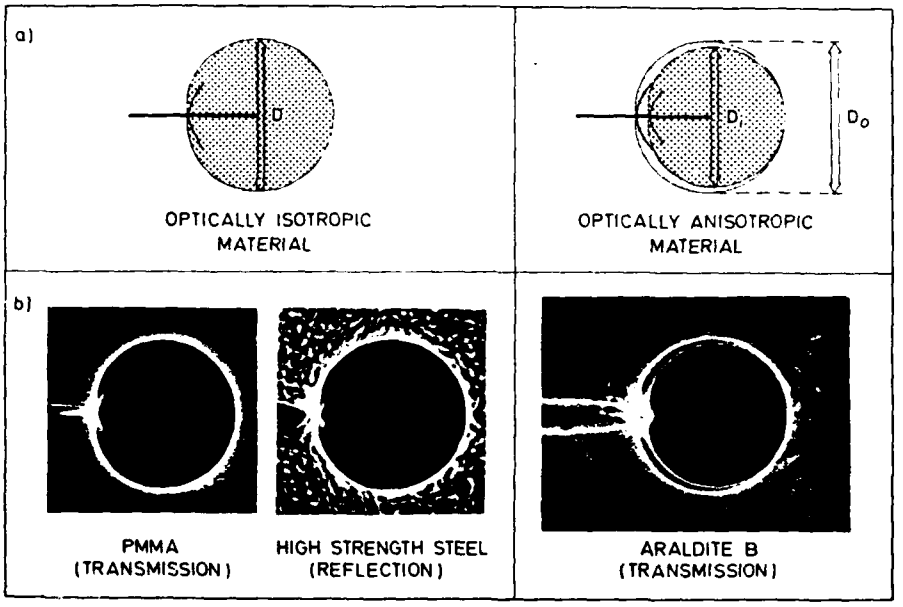

Fig. 6 Mode I caustics, a) calculated, b) measured

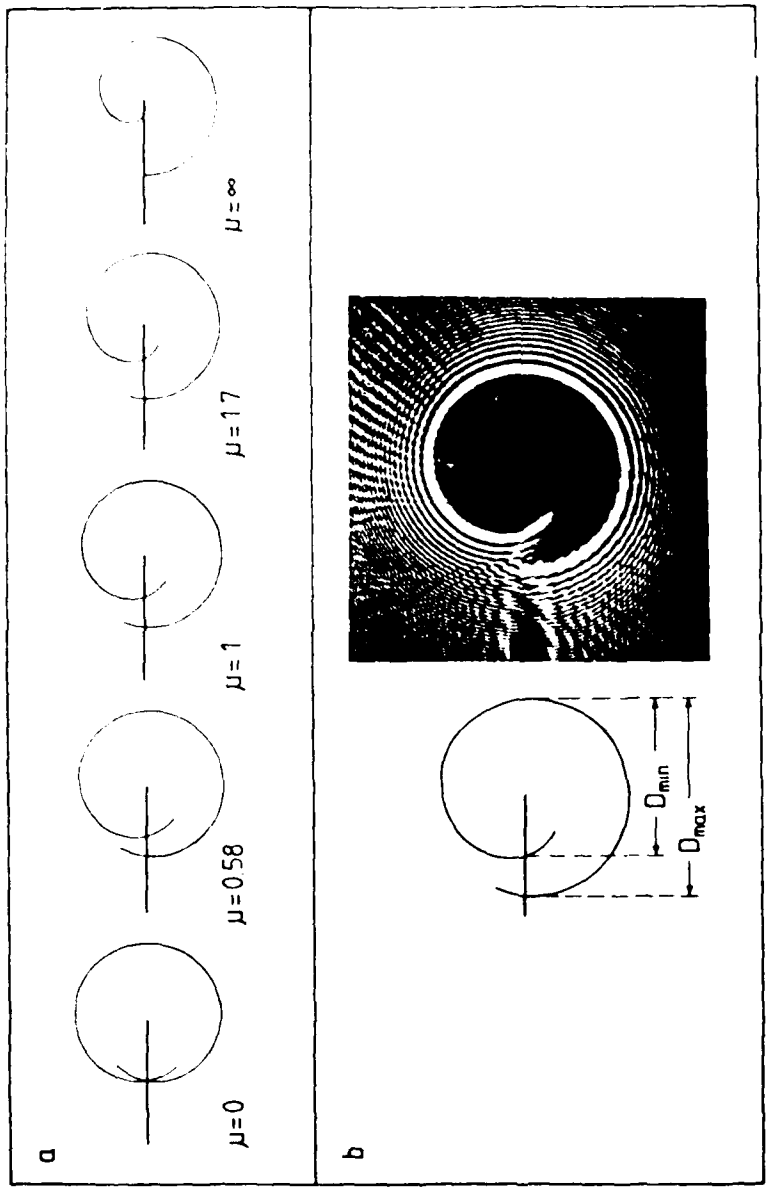

Fig. 7 Mixed (I, II) mode caustics, a) calculated for different ratios $\mu = K_{II}/K_I$, b) definition of diameters and experimentally observed shadow pattern

$$K_i = M_{i,k} \cdot D_k^{5/2} \qquad (i, = I,II;\ k = min, max). \qquad (2)$$

This relation is similar to eq.(1). The (four possible) factors $M_{i,k}$ which again contain optical and geometrical parameters are known functions [39-41].

For further details of the shadow optical techniques see [32,33,41]. Crack tip caustics are of a simple form and can easily be evaluated. The technique, therefore, is very well suited for investigating complex phenomena, as e.g. in fracture dynamics, and is used in this work to measure dynamic stress intensity factors under impact loading.

2.3 Research Program

The goal of the first year's research effort was to build up the experimental set-up and to perform preliminary experiments in order to test the measuring system. On the basis of these experiments data should be generated to specifiy the parameters for the subsequent main investigations scheduled for the second and the third year of the research project.

3 DESIGN AND BUILDING OF THE EXPERIMENTAL SET-UP

The IWM-gas gun is used for impact loading of the specimens. A schematic drawing and a photograph of the equipment are given in Fig. 8. The high pressure chamber (30 l volume) can be filled with air or helium to a maximum pressure of 200 bar. A barrel of 50 mm diameter and 3 m length is used to accelerate the projectile. A measuring chamber at the muzzle holds the target and the measuring devices. The catcher tank collects the remaining pieces of the experiment and is able to absorb their kinetic energy. The gas gun has been modified and supplemented by special devices in order to meet the specific requirements for the proposed experiments. Shadow optical pictures of the specimen during impact are recorded with a Cranz-Schardin high speed camera. 24 pictures can be taken at a minimum picture interval time of 1 µs. A photograph of the camera is given in Fig. 9. An overview of the complete experimental set-up is given in Fig. 10. In particular the following work has been performed:

- Design and construction of a holding fixture for the specimens: Special arrangements have been developed to load the specimens in either one of the two loading conditions, i.e. direct impact loading and base plate loading. These arrangements meet the optical requirements for a photographic recording of the specimen behavior. Illustrative views of the two loading arrangements are given in Figs. 11 and 12.

For the conditions of direct impact loading the specimen is positioned at the center line of the gas gun. The specimen is almost free and only loosely attached to a support (just to keep it in a definite position).

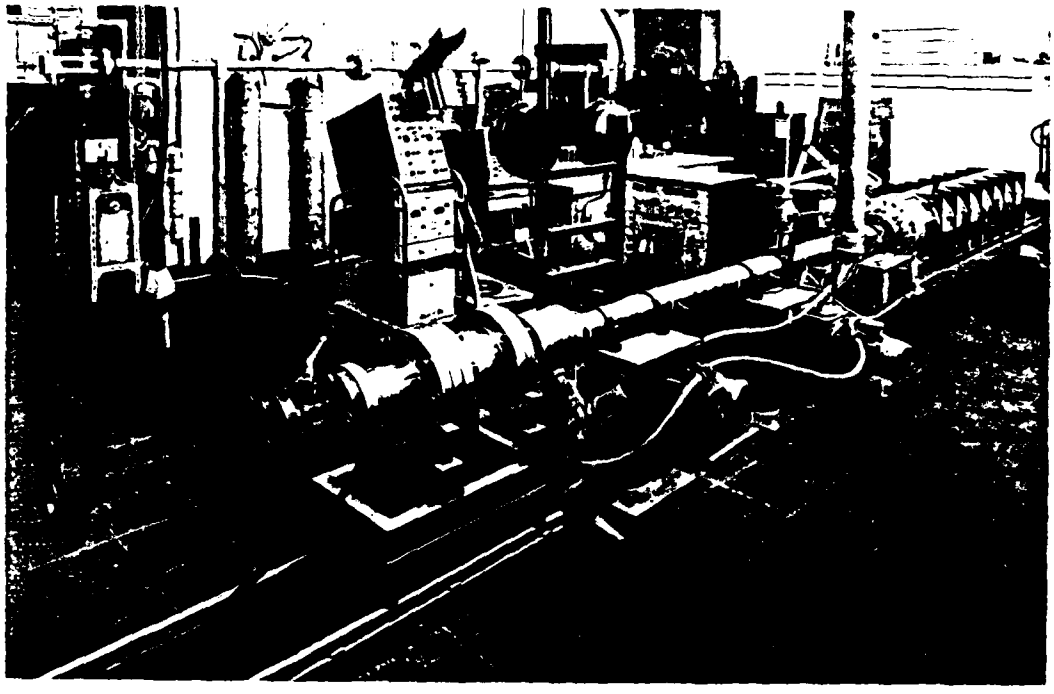

DRUCKKAMMER		LAUF		MESSKAMMER mit AUFFANGER	
Volumen	1 ... 30 l	Länge	3 m	Länge	2 m
p_{max}	200 bar	Kaliber	50 mm	Volumen	120 l
		Volumen	6 l		

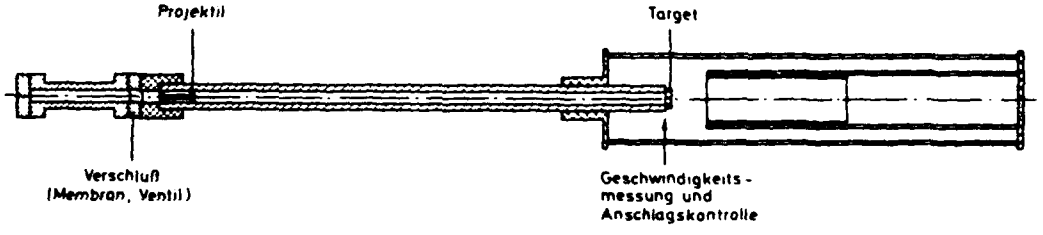

Fig. 8 IWM gas gun

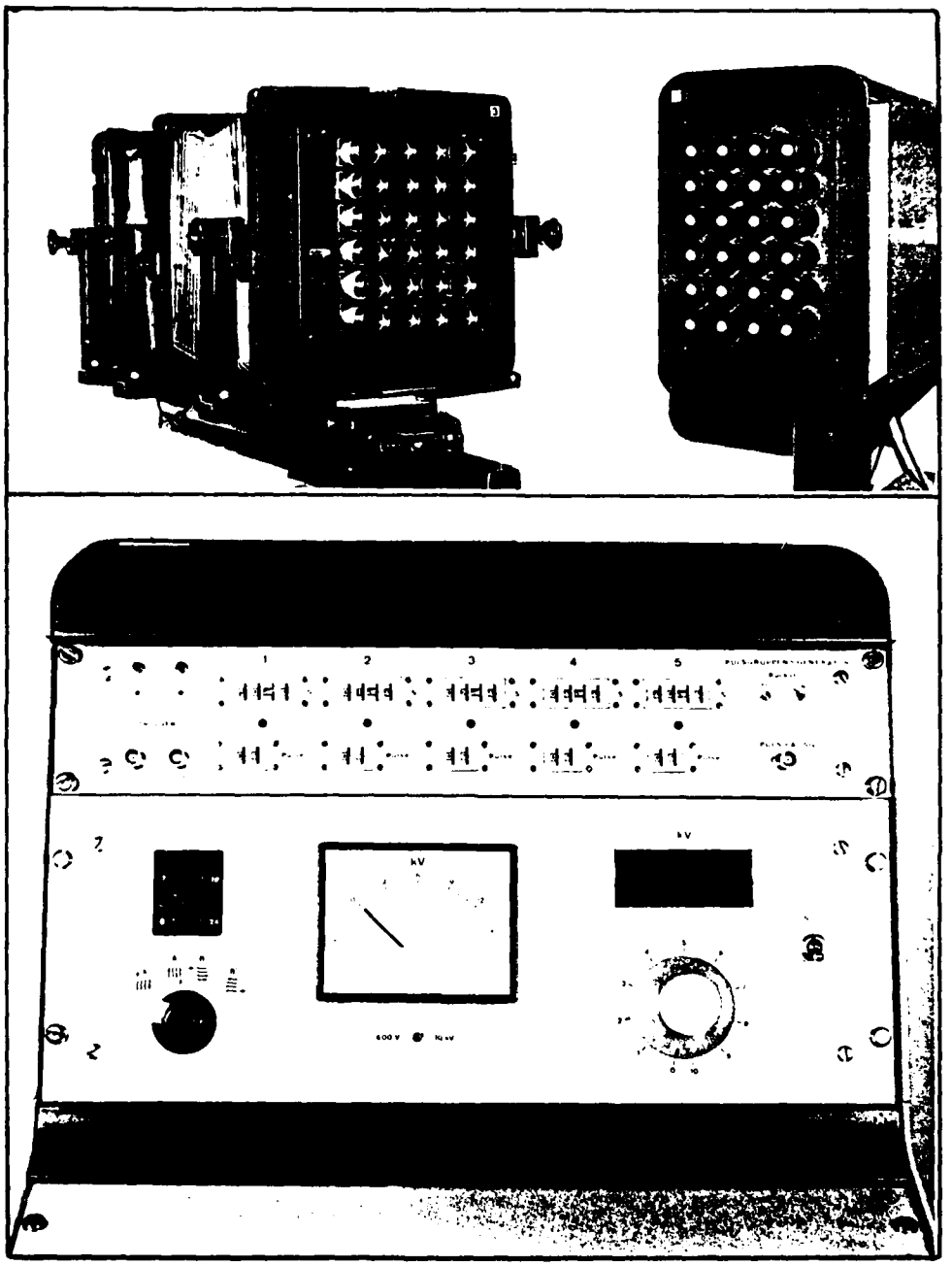

Fig. 9 Cranz-Schardin 24 spark high spead camera

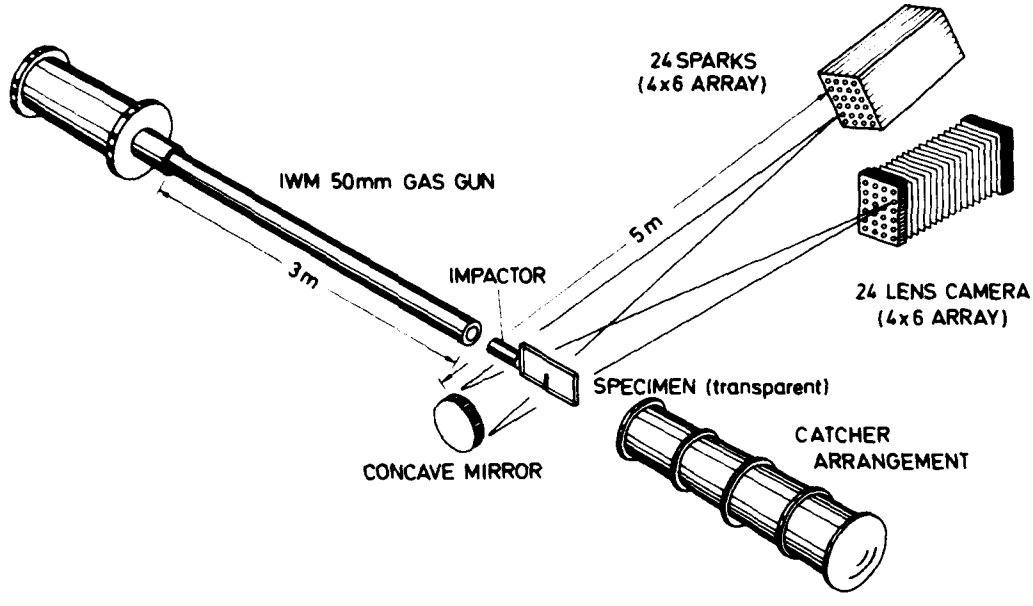

Fig. 10 Experimental set-up, schematically

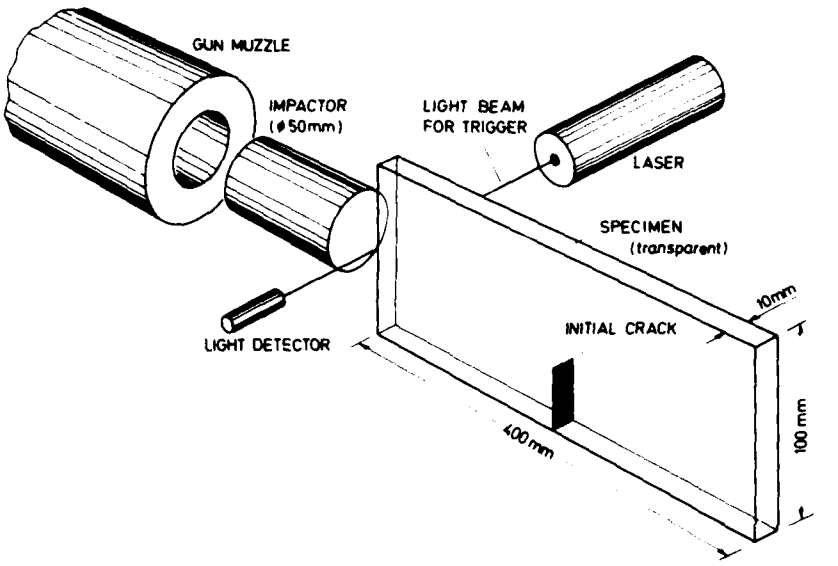

Fig. 11 Illustrative view of the direct impact loading arrangement

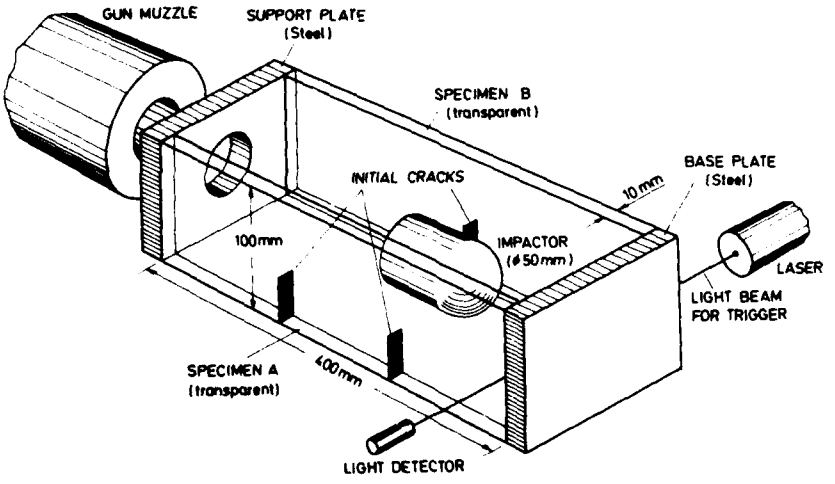

Fig. 12 Illustrative view of the base plate loading arrangement

For the conditions of base plate loading an arrangement with two specimens has been developed. The specimens are positioned to the right and to the left hand side of the center line of the gas gun. The front ends of the specimens are attached to a rigid support plate which is kept at a fixed position. The ends of the specimens are fastened to a free base plate which is accelerated by the impinging projectile. The observation direction of the shadow optical measuring system is perpendicular to the surfaces of the specimens. Thus, the two specimens - one lying in front of the other - are simultaneously photographed when the shadow optical system is used in transmission with transparent specimens. The arrangement then has the advantage that two different crack configurations can simultaneously be investigated in the two specimens. Of course, only one specimen is analyzed if the shadow optical system is used in reflection with steel specimens.

A fixture to hold the specimens according to these two arrangements has been designed and built. A photograph is given in Fig. 13. The fixture consists of two parts: a front part and a rear part which are separately mounted on a supporting I-beam (180 mm high, 3400 mm long). The distance between the two parts can be varied, thus specimens of different length can be utilized in the experiments. The maximum specimen width is limited to 100 mm. The front part of the fixture is adjustable to allow for a straight and plane impact.

• Catcher tank:
An existing catcher tank has been modified and adapted to the loading fixture and the supporting I-beam. The catcher arrangement is necessary in order to collect the moving parts after impact, i.e. the projectile, the base plate, the broken pieces of the specimen etc. Rags absorb the kinetic energy of the moving parts.

• Triggering device for the high speed camera:
An optical device has been designed and built to trigger the Cranz-Schardin high speed camera. A laser beam traverses the path of the flying projectile (see Figs. 11 and 12)
- directly in front of the specimen (direct impact condition) or
- directly in front of the base plate (base plate loading condition).
The laser beam is interrupted by the impinging projectile and thus provides a pulse to trigger the camera via a delay time generator.

• Adaption of the Cranz-Schardin high speed camera:
The 24 spark high speed camera has been adjusted and aligned to the gas gun. Since the camera is normally operated at a height of about 1.4 m, the gas gun, however, at a lower height of only 0.6 m, considerable work was necessary to lower the whole optical arrangement, i.e. the camera, the spark unit and the mirror. The existing tripods had to be modified by special holding fixtures.

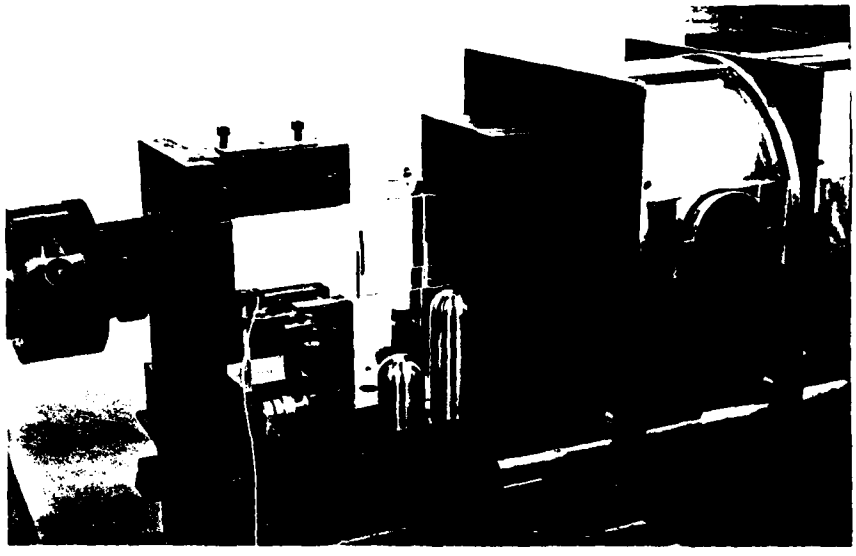

Fig. 13 Holding fixture for specimen

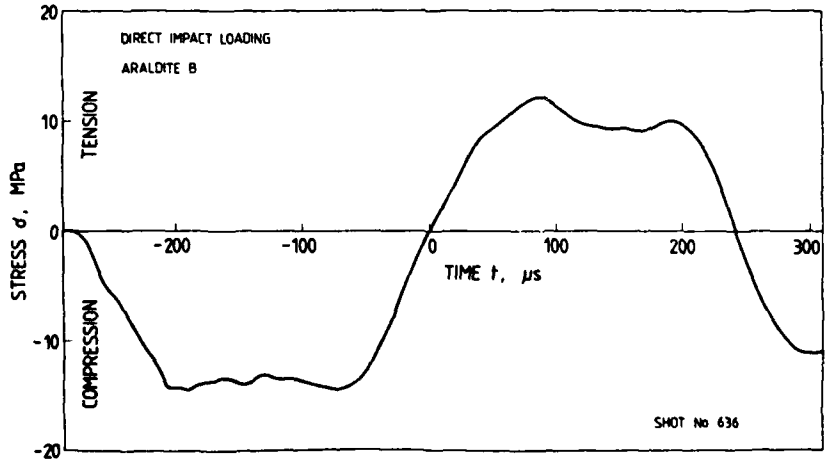

Fig. 14 Stress pulse history

4 TEST OF THE EXPERIMENTAL SET-UP

Several shots have been performed to test the different systems of the experimental set-up, in particular
- the holding fixture and the catcher tank,
- the triggering system, and
- the alignment of the high speed camera.

The information obtained from these preliminary experiments was used to improve the experimental set-up. Modifications to the first design of the holding fixture were necessary in order to achieve an undisturbed tensile loading of the specimens under the two loading conditions. Serious difficulties were encountered with the triggering system. In several cases the air shock wave travelling ahead of the flying projectile provided the first trigger pulse. Concequently the camera was started ahead of time. These problems have been solved by adjusting the trigger threshold to an appropriate level. This level has experimentally been established in a series of test shots. The final alignment of the high speed camera caused no major problems.

Results obtained under the two different types of loading conditions are reported in the following sections. Due to cost reasons, these experiments were performed with specimens made from the model material Araldite B.

4.1 Direct Impact Loading

First, several experiments have been performed to study the load pulse history in the specimen under direct impact loading conditions (see Fig. 11). Data were obtained from strain gage measurements, photoelastic investigations, and shadow optical investigations. Some typical results which give an indication of the loading situation in the specimens are reported.

4.1.1 Load Pulse History

All experiments were performed with specimens 400 mm long and 100 mm wide. The specimen thickness was 10 mm. The specimens were impacted by a projectile of 200 mm length and 50 mm diameter made from the same material as the specimens, i.e. Araldite B. The chosen dimensions were a result of pre-experiments in which the length of the specimen has been varied: With short specimens, i.e. specimens of length 100 mm and 200 mm it was found that the crack did not propagate in a straight manner through the sepcimen but deviated from its original direction. Test specimens of 400 mm length, however, showed a straight crack propagation in the original crack direction.

- Strain Gage Measurements:

The signal from a strain gage positioned in the middle of a specimen without a crack is shown in Fig. 14. For a period of 280 µs the crack is loaded by compressive stresses, then tensile stresses build up due

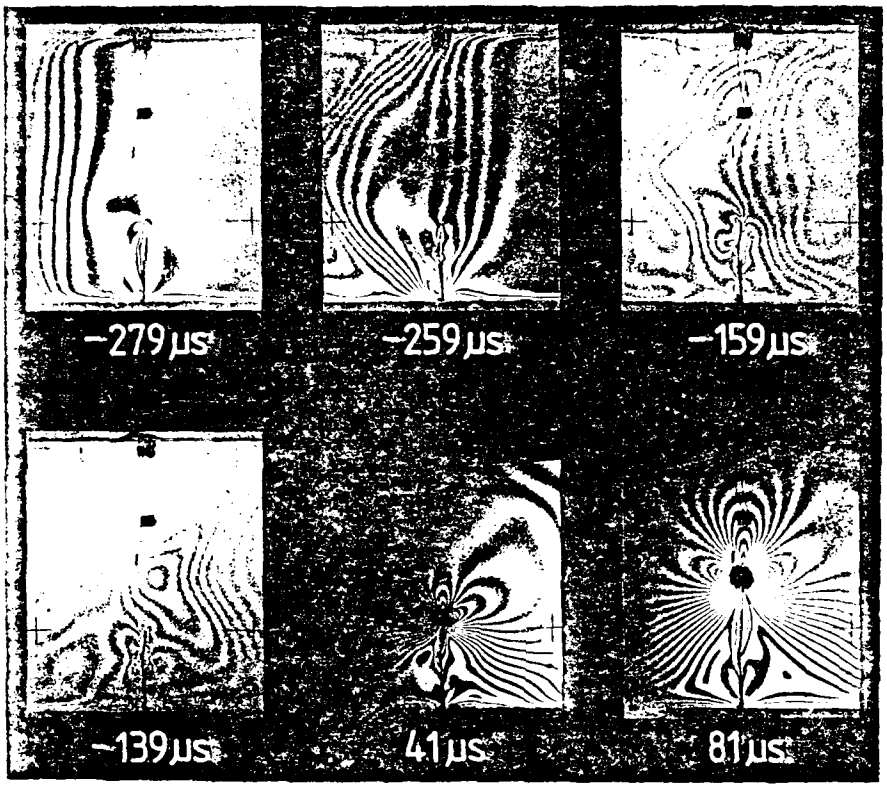

Fig. 15 Photoelastic recording of the passage of the stress pulse through the specimen

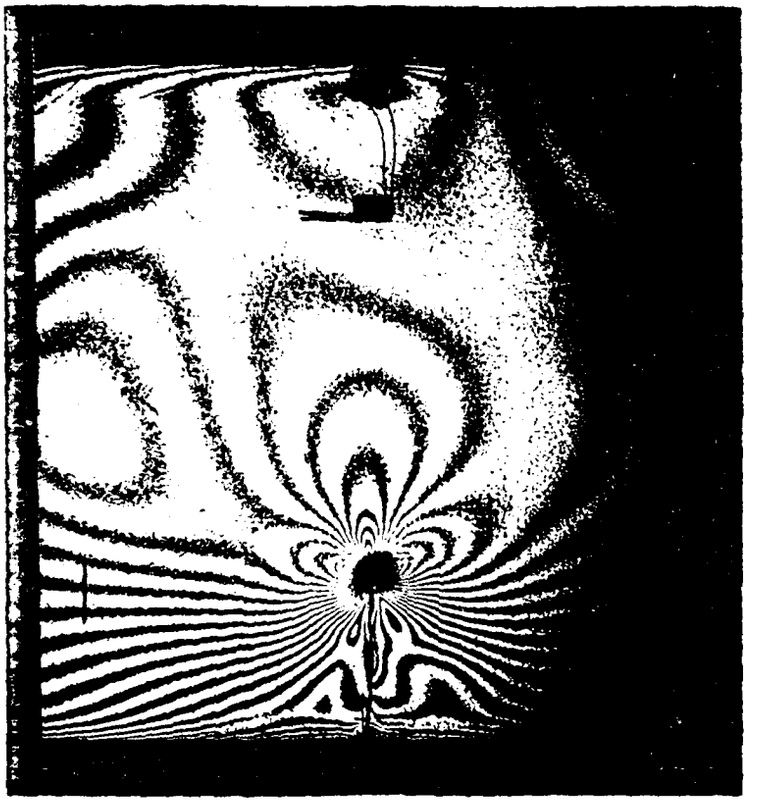

Fig. 16 Photoelastic crack tip fringe pattern

to the reflection of the compressive waves at the free ends of the specimen and the projectile. In this diagram and also in the following ones the time at which compression changes into tension has been set equal to zero (0 μs). The tensile stress pulse has a duration of about 240 μs. At later times compressive stresses again build up in the center part of the specimen. The increasing part of the tensile stress pulse would be used in specimens with initial cracks to initiate unstable crack propagation.

In order to get information on the stress history not only at the single point of a strain gage but over a larger area further investigations have been carried out utilizing photoelastic and shadow optical techniques.

- Photoelastic Measurements:

Photoelastic isochromatic fringe patterns associated with the passage of the stress pulse through the specimen were recorded. The Cranz-Schardin camera was equiped with a photoelastic measuring device and focussed directly on the specimen. The specimen dimensions and the impact conditions were the same as for the strain gage measurements, but specimens with initial cracks were utilized. Fig. 15 shows six pictures at subsequent times. The passage of the compressive stress pulse into the specimen is visible. Since the crack is closed by the compressive stresses the stress pulse is only slightly disturbed by the crack. After tensile stresses have been built up in the center part of the specimen ($t > 0$ μs), the typical tensile crack tip fringes develop. Fig. 16 shows another photoelastic picture of a tensile crack tip fringe pattern.

No attempts have been made to quantitatively evaluate the rather complex photoelastic fringe patterns; instead a special shadow optical measuring technique was utilized to obtain information on the stress distribution in the specimen.

- Measurement of Shadow Patterns around Hole Fields:

Shadow patterns around holes which are drilled into a specimen can be used as indicators of the stress field at that point. Fig. 17 shows the shadow pattern around a hole under the influence of a biaxial stress field $\sigma_y = p$, $\sigma_x = q$, with $p > q$ (see [30]). The intersection of the shadow pattern is oriented parallel to the larger of the tensile stresses. The diameter of the caustic D in longitudinal direction of the shadow pattern is quantitatively related to the difference of the principle stresses $p - q$,

$$p - q = N \cdot D^4. \qquad (3)$$

N is a known numerical factor which depends on the optical arrangement and the material utilized. Consequently, for a tensile stress field the intersection of the shadow pattern points into the direction of the stresses, for compressive stress fields it points in a direction per-

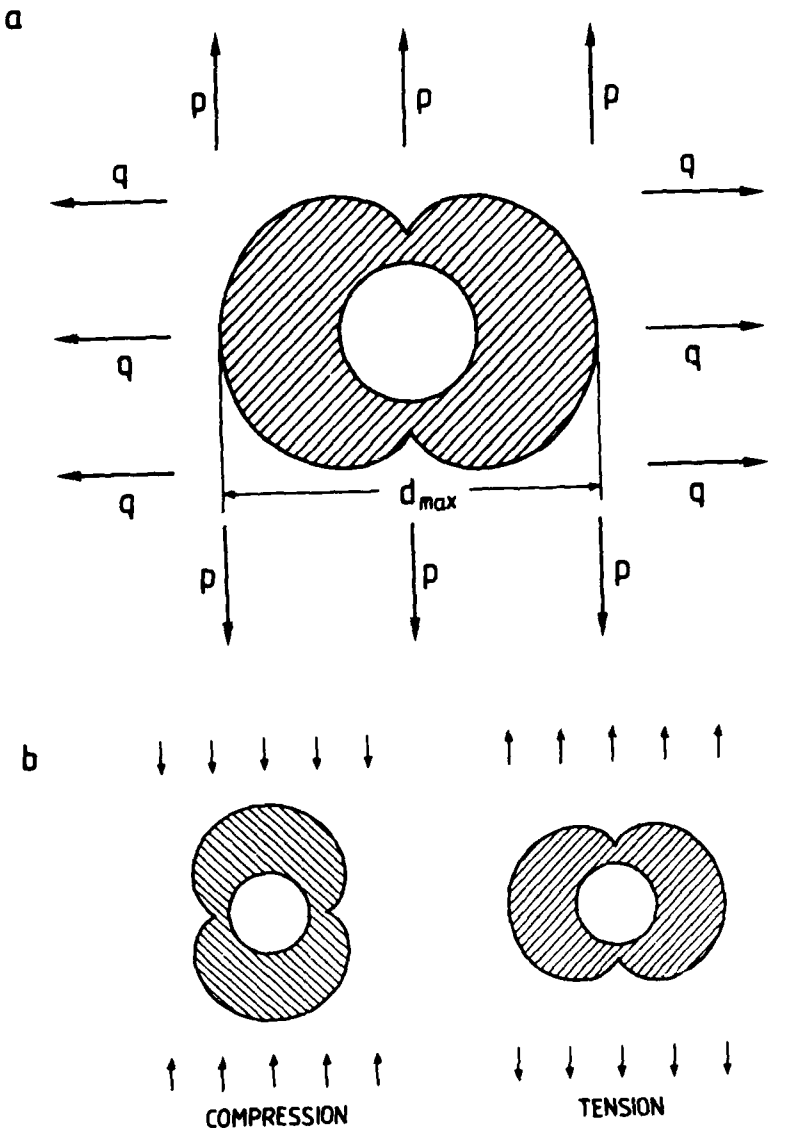

Fig. 17 Caustics around a hole

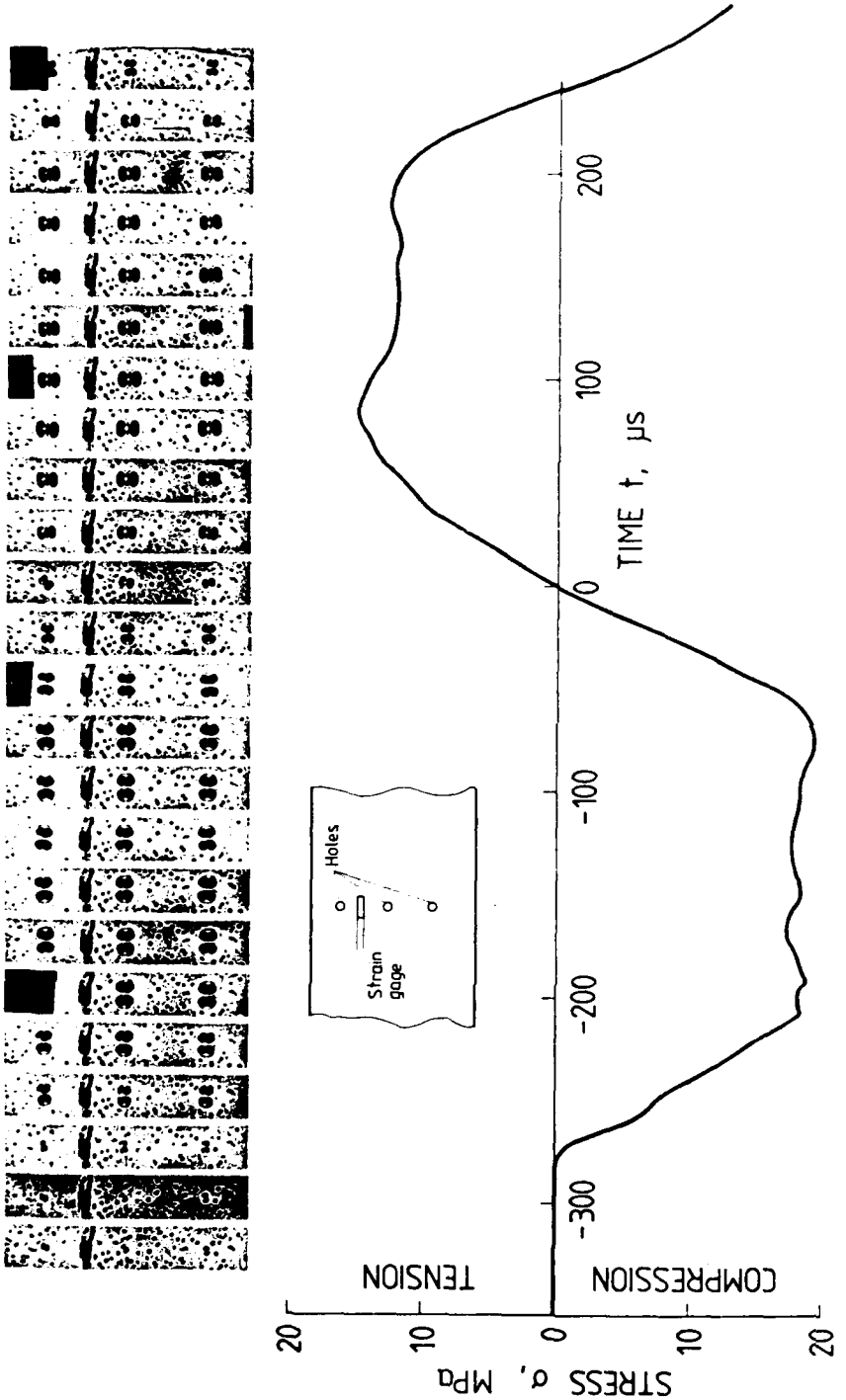

Fig. 18 Shadow optical investigation of the stress pulse history, (arrangement of 3 holes)

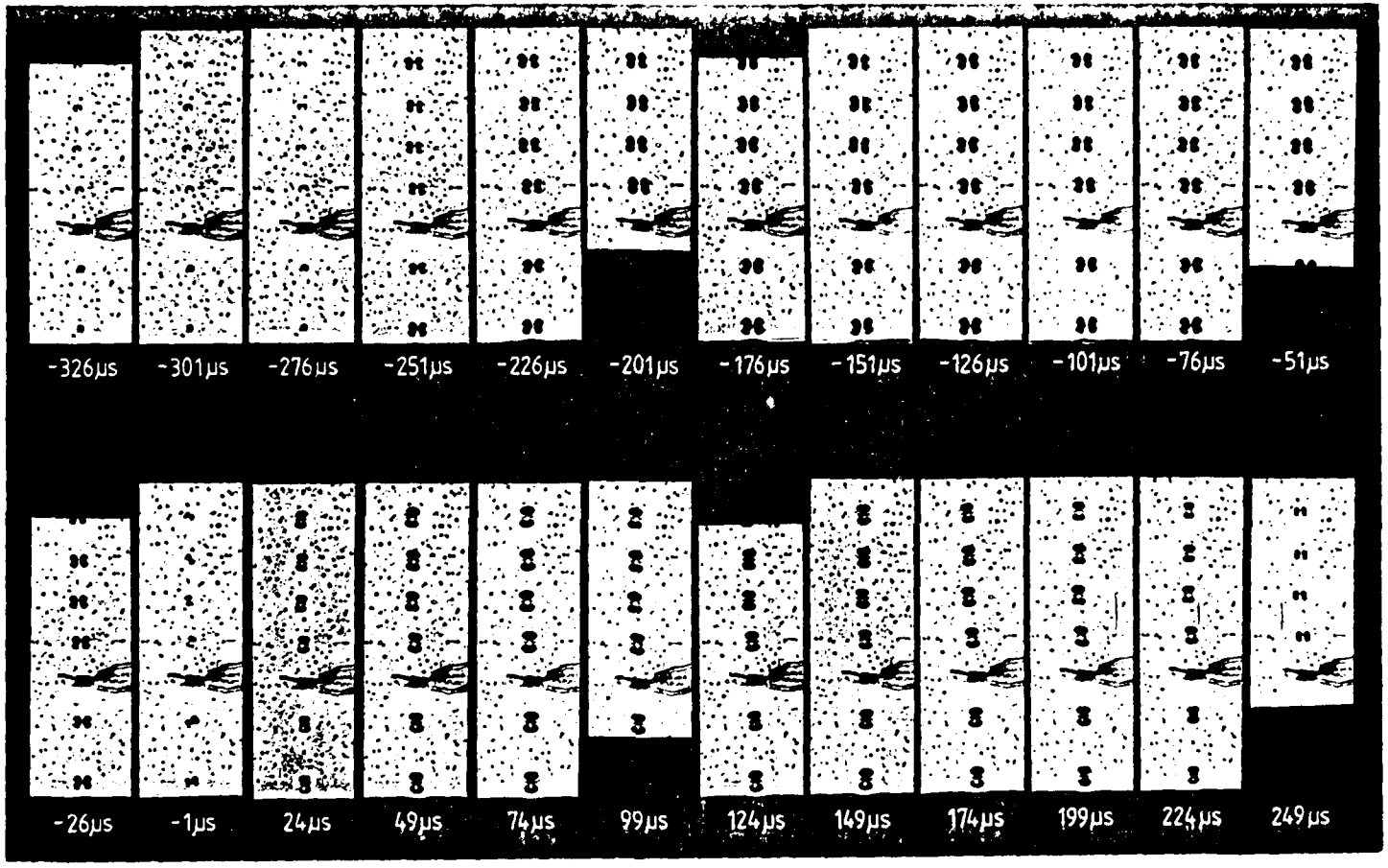

Fig. 19 Shadow optical investigation of the stress pulse history, (arrangement of 6 holes)

pendicular to the stress field. Furthermore, the size of the caustic is an indicator of the magnitude of the stress. Utilizing this technique, a series of experiments has been performed to study the stress distribution in the specimen.

First, a row of three holes was drilled in the middle of the specimen at 1/4, 1/2, and 3/4 of the width of the specimen. In addition, the specimen was instrumented by a strain gage located between two of the holes. The insert in Fig. 18 illustrates the geometrical arrangement. The results of both, the strain gage measurements and the shadow optical investigations are given in Fig. 18. The shadow patterns change their direction and their size analogous to the strain gage signal. The size of the patterns varies with the stress amplitude. In picture No. 14 the direction of the patterns change and from picture No. 16 on tensile shadow patterns are recorded. The last pattern at 250 µs again indicates compressive stresses.

More detailed information on the distribution of the stresses along the width of the specimen is obtained from the results in Fig. 19. In this experiment six instead of three holes were used. The picture shows the same general behavior as discussed above. The six shadow optical patterns positioned across the width of the specimen do not vary very much in size, in particular the patterns near the boundary are almost of the same size as the center patterns, indicating a rather even distribution of stresses along the location of the prospective crack.

The passage of the stress pulse through the specimen has been made visible in a specimen with a row of holes positioned in length direction of the specimen. The shadow optical pictures are given in Fig. 20. Pictures No.1 to 13 show the propagation of the compressive stress pulse into the specimen. Between pictures No. 13 and No. 14 the stresses change from compression into tension and between pictures No. 23 and No. 24 they have changed back again into compression. Fig. 21 shows the change from the compressive state of stress to the tensile stresses with higher time resolution. In this case a cross shaped arrangement of holes has been utilized. At 0 µs zero stresses are observed directly in the center of the specimen, the region around this center still is under compressive stresses. In the next picture, at 18 µs, tensile stresses have already built up in the center.

An overview on the stress distribution in the whole specimen is given in Fig. 22, showing the shadow optical photograph of a specimen with a field of 91 holes. The photograph was taken during the tensile loading phase. The data indicate that the stress field in the center of the specimen, i.e. at the location of the prospective crack, is rather uniform, thus allowing a controlled investigation of the instability behavior of cracks.

In a subsequent experiment the development of the stress intensification at an initial notch has been photographed. A notch of 35 mm length has been machined in the specimen which had been provided with the hole

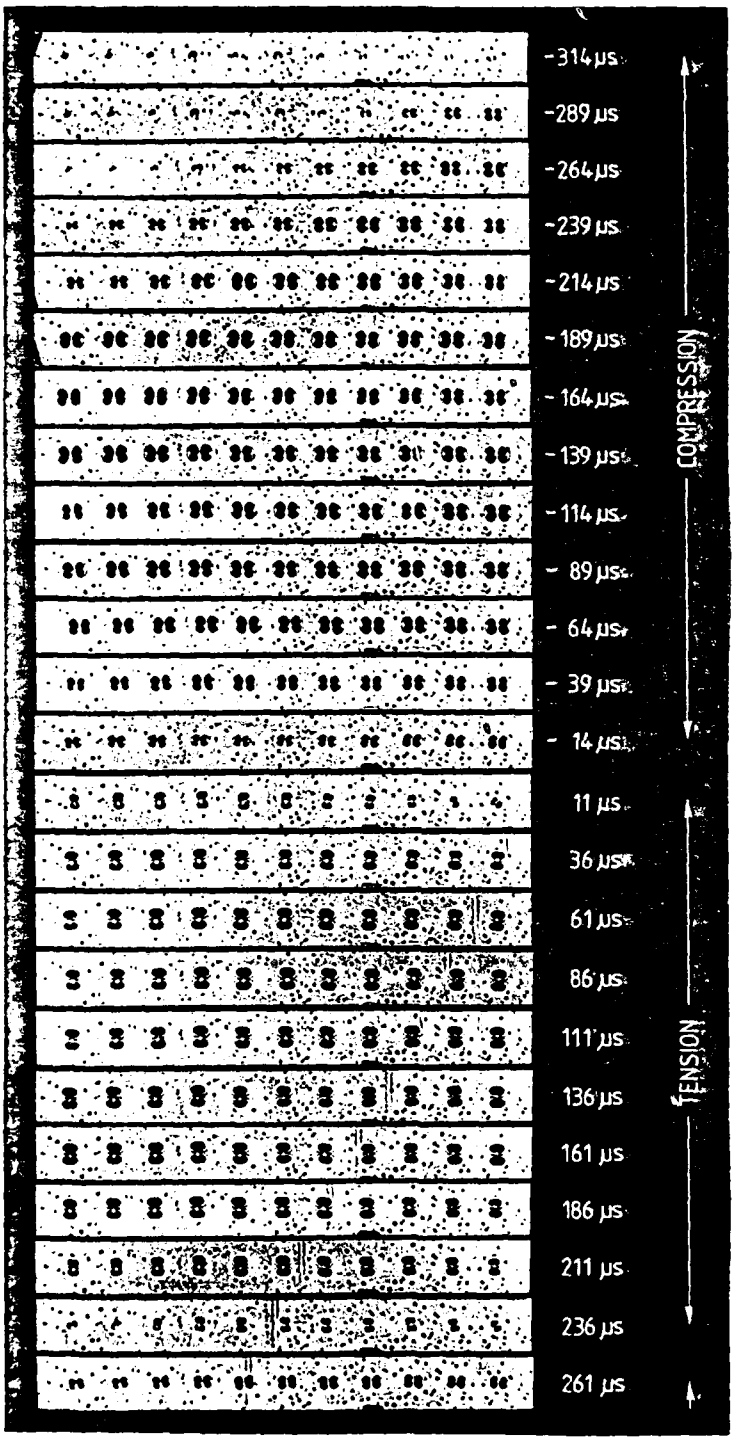

Fig. 20 Shadow optical investigation of the stress pulse history, (arrangement of holes in length direction of the specimen)

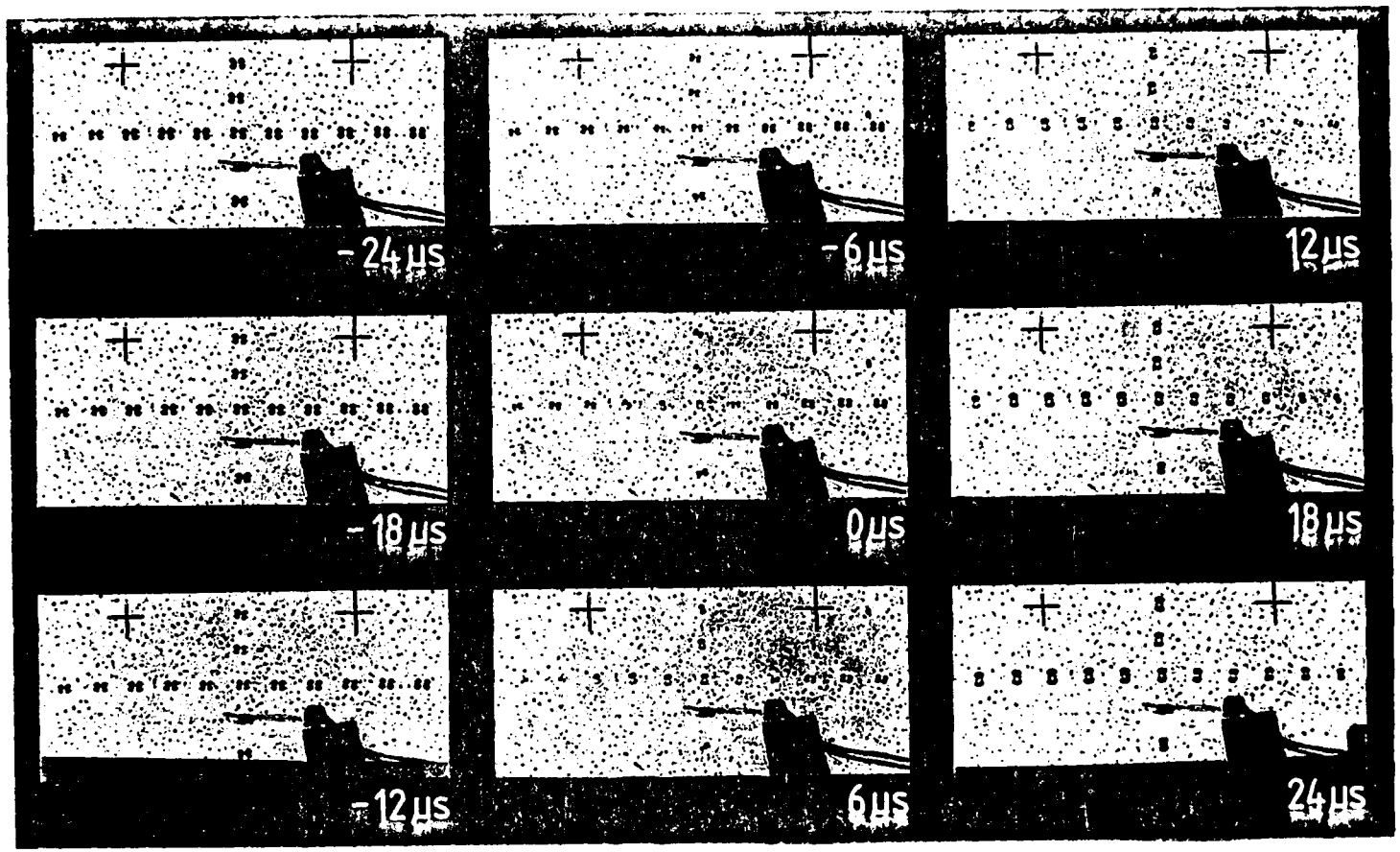

Fig. 21 Change from compressive to tensile stresses (shadow optical investigation with a cross shaped arrangement of holes)

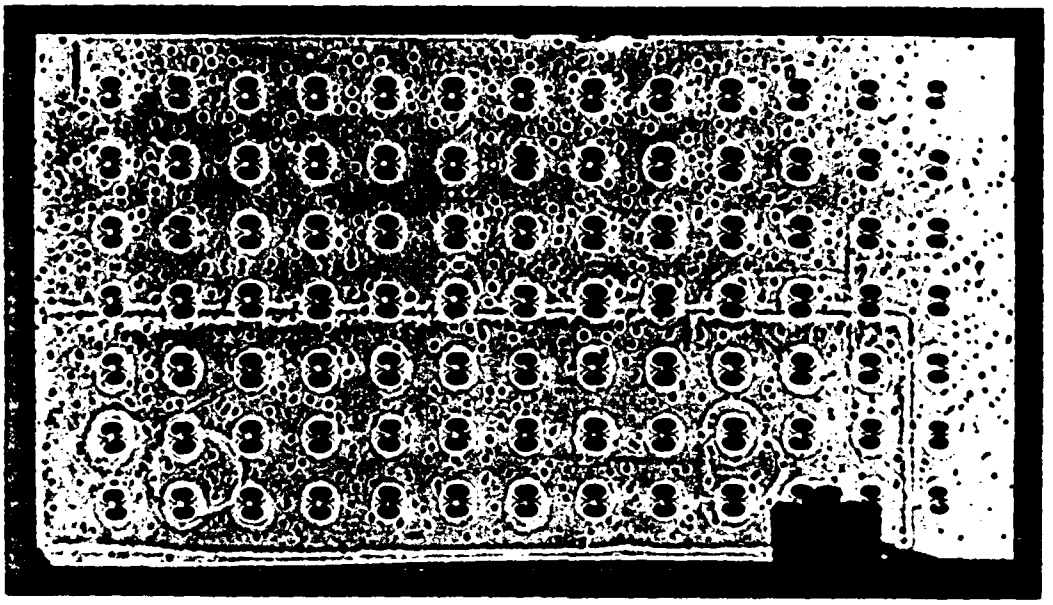

Fig. 22 Distribution of tensile stresses in the specimen (shadow optical investigation with a hole field)

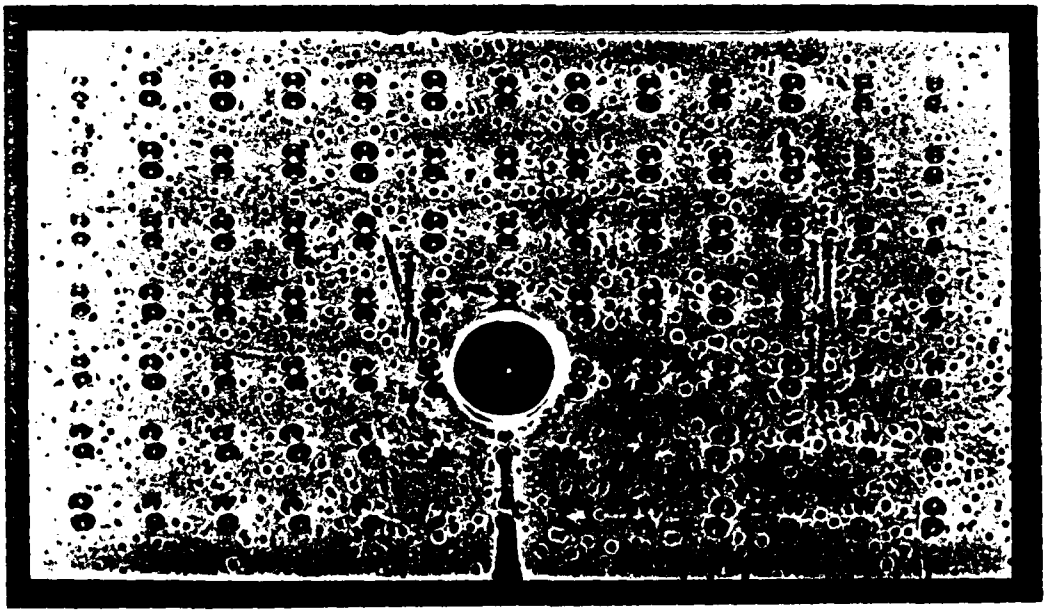

Fig. 23 Crack tip caustic and caustics of a hole field under tensile loading

field already. Fig. 23 shows a well developed mode-I caustic around the crack tip. The picture was taken 54 μs after the beginning of the tensile stress field. The shadow patterns around the holes behind the crack tip indicate unloading of the specimen in this area. The other patterns in the near crack tip region show a disturbed stress field due to interactions with the crack tip stress field.

The complete history of the crack tip stress intensification from the beginning of the impact process on is shown in Fig. 24. A specimen with a sawed in initial notch has been utilized in the experiment. Since the surfaces of the notch could not come into contact with each other during the compressive loading phase a compressive stress intensification (negative stress intensity factor K_I) builds up first, as is indicated in pictures No. 1 to 8. These compressive crack tip caustics then disappear when the tensile loading phase starts at 0 μs and change into tensile crack tip caustics.

The crack tip caustics observed in Figs. 23 and 24 are of good quality and any difficulties in analyzing these shadow patterns are not expected.

4.1.2 Crack Instability Experiments

A series of experiments has been performed to generate the first instability data and to find the appropriate impact parameters for the main investigations. Specimens with initial cracks of different lengths were prepared the following way: A notch of length less than the desired length has been sawed into the specimen. This notch was subsequently extended in length by precracking using a wedge loading device. In order to allow for an undisturbed passage of the compressive stress pulse across the crack, a plate of thickness equal to the width of the notch was inserted into the notch.

The results of a typical experiment are shown in Figs. 25 and 26. In Fig. 25 twelve of a series of 24 shadow optical pictures are reproduced. The camera has been delayed by an appropriate time to only analyze the shadow pattern under tensile loading. The pictures No. 1 to 4 show the increase of the dynamic stress intensity factor at the tip of the stationary crack. At picture No. 5 the crack has become unstable. Pictures No. 6 to 12 show the propagating crack. Due to the sudden acceleration of the crack tip, relief waves are radiated from the crack tip into the specimen which were visible in some of the photographs.

Fig. 26 shows quantitative data obtained according to eq. (1) from the shadow optical photographs. The dynamic stress intensity factor, K_I^{dyn}, and the momentary position of the crack tip, a, are plotted as functions of time. The a(t)-data give an indication of the time at which the crack becomes unstable. With this information the interesting parameters can be determined: The critical stress intensity factor for onset of rapid crack propagation, i.e. the dynamic fracture toughness, K_{Id}; the time to fracture, t_f; and the effective stress intensification rate, $\dot{K}_I^{dyn}$.

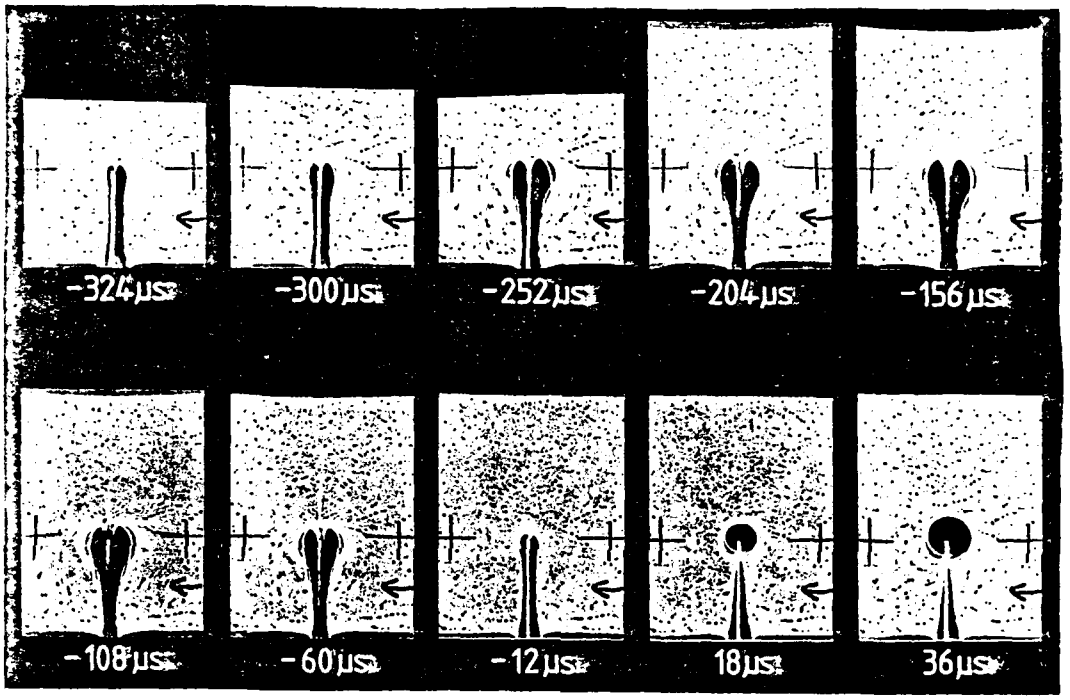

Fig. 24 Complete listing of compressive and subsequent tensile crack tip caustics

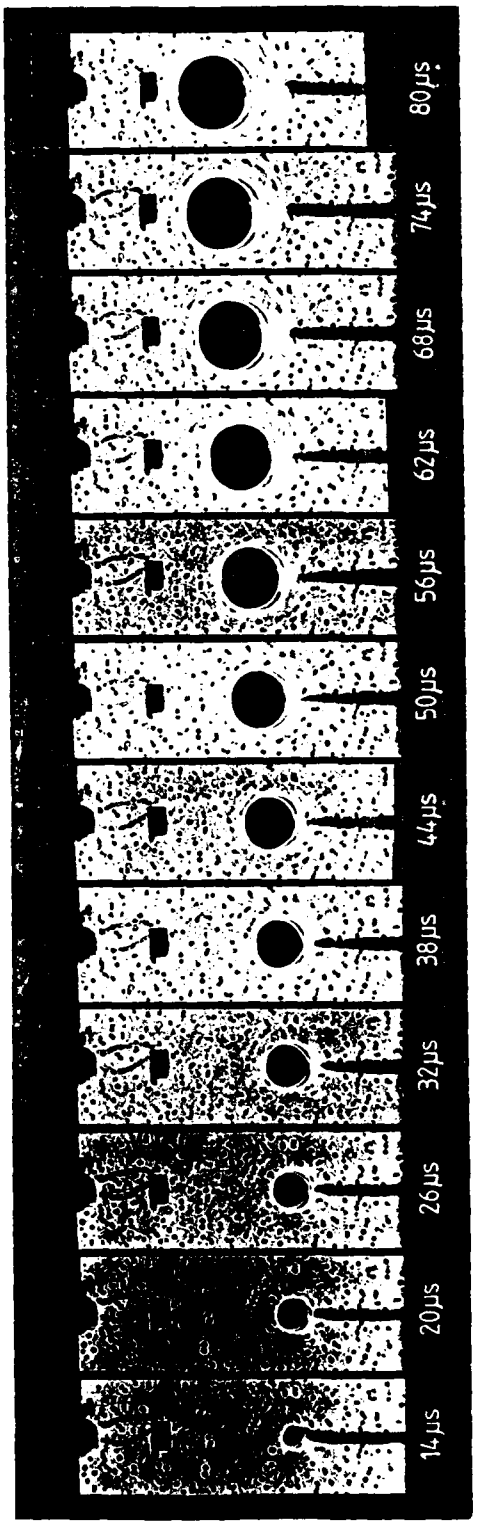

Fig. 25 Crack tip caustics, single crack under direct impact loading

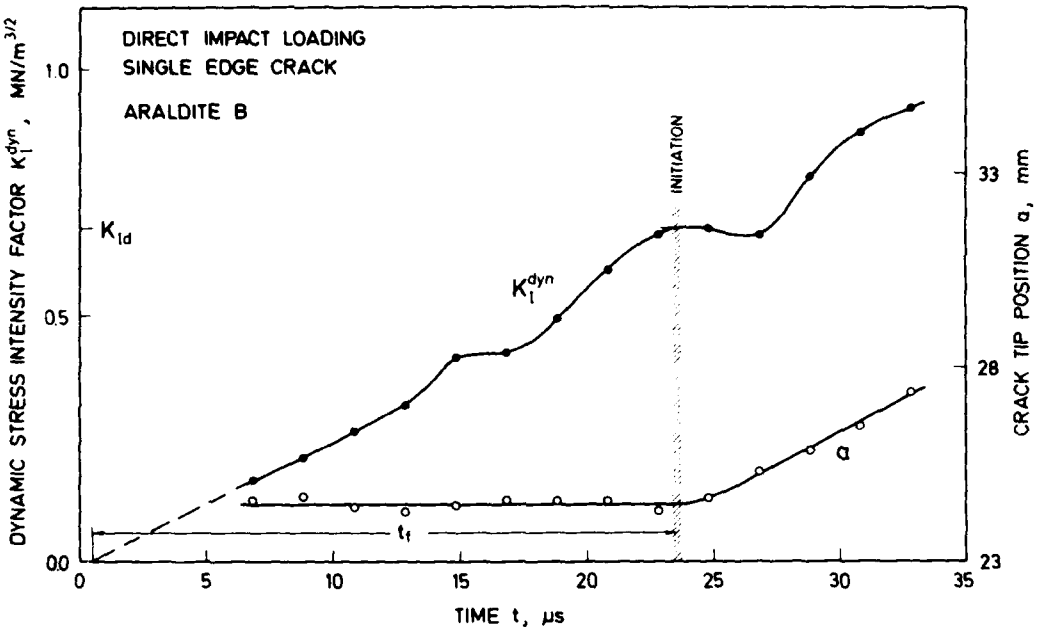

Fig. 26 Dynamic stress intensity factor and crack tip position, direct impact loading

At velocities higher than about 40 m/s damage of the specimen under the contact area with the projectile was observed. The maximum allowable impact velocity for the direct loading arrangement, therefore, is in the range of 40 m/s. The stress intensification rate for specimens of the given size and material accordingly is of the order of 10^5 $MNm^{-3/2}s^{-1}$. The limited velocity of course will be considerable larger when steel specimens will be investigated at the end of the research project.

4.2 Base Plate Loading

Since the stress distribution in the specimen under base plate loading conditions is much simpler than under direct impact conditions a detailed investigation of the distribution of stresses in the specimens has not been considered necessary. The loading arrangement has been tested by directly performing impact experiments with pre-notched or pre-cracked specimens.

To allow for a comparison with the direct impact data the specimen dimensions have been chosen the same as for the direct loading experiments, i.e. the specimens were 400 mm long, 100 mm wide and 10 mm thick. Two specimens were simultaneously tested in the dual specimen loading fixture. Different crack configurations were utilized for the two specimens. Usually one of the specimens contained a single crack, whereas the other specimen contained a double crack configuration. The two specimens were fastened to a steel base plate (100 x 100 mm^2, 20 mm thick, 1.6 kg mass) which was impacted by steel projectiles of 50 mm diameter and different lengths.

Typical results are shown in Figs. 27, 28 and 29. Fig. 27 shows a series of shadow optical photographs. It shall be emphasized again that these pictures do not show one specimen with a configuration of three cracks, but two specimens, one with a single crack (i.e. the middle crack in the photographs) and one with a double crack configuration (i.e. the outer cracks in the photographs). The tensile stress pulse impinges on the cracks from the right hand side. The crack which is loaded the longest time exhibits the largest stress intensity factors. The shadow patterns of the middle crack and of the left hand crack (at least at early times) are of pure mode-I type. The shadow pattern of the right hand crack shows a mixed mode loading from the very beginning on, since this crack is influenced by the left hand crack tip stress field. In picture No. 11, at 110 µs, the left hand crack becomes unstable and propagates through the specimen. Later on, at 150 µs, the center crack (i.e. the single crack in the other specimen) becomes unstable. The single crack propagates along its original direction without any deviation. The path of the left hand crack shows a slight deviation from the original crack direction, indicating a small superimposed mode-II loading. The observed experimental findings are in accordance with expectations.

Quantitative data for the single crack are shown in Fig. 28. The dynamic stress intensity factor, K_I^{dyn}, and the momentary crack length, a,

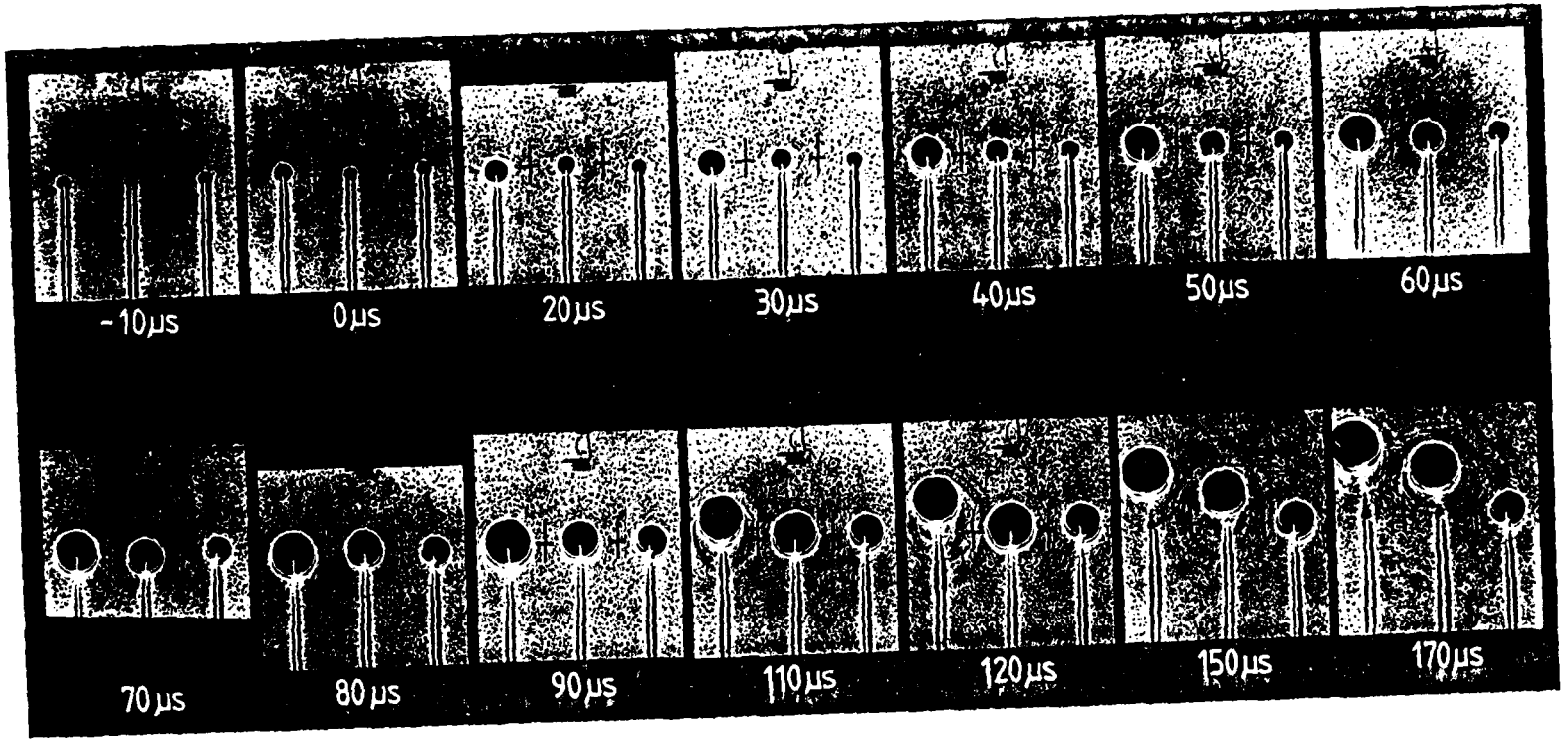

Fig. 27 Crack tip caustics, a single crack (inner) and a double crack configuration (outer cracks) under base plate loading

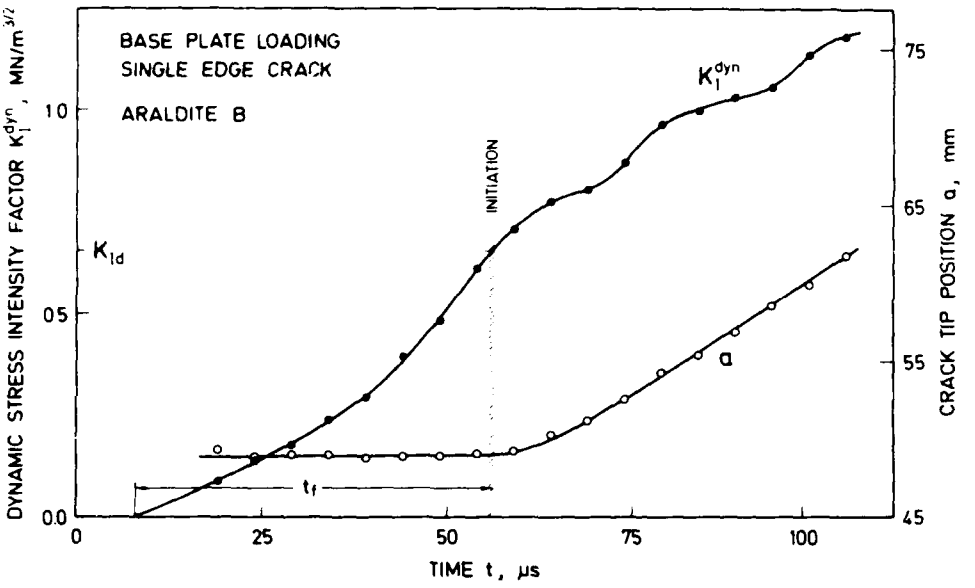

Fig. 28 Dynamic stress intensity factor and crack tip position, base plate loading

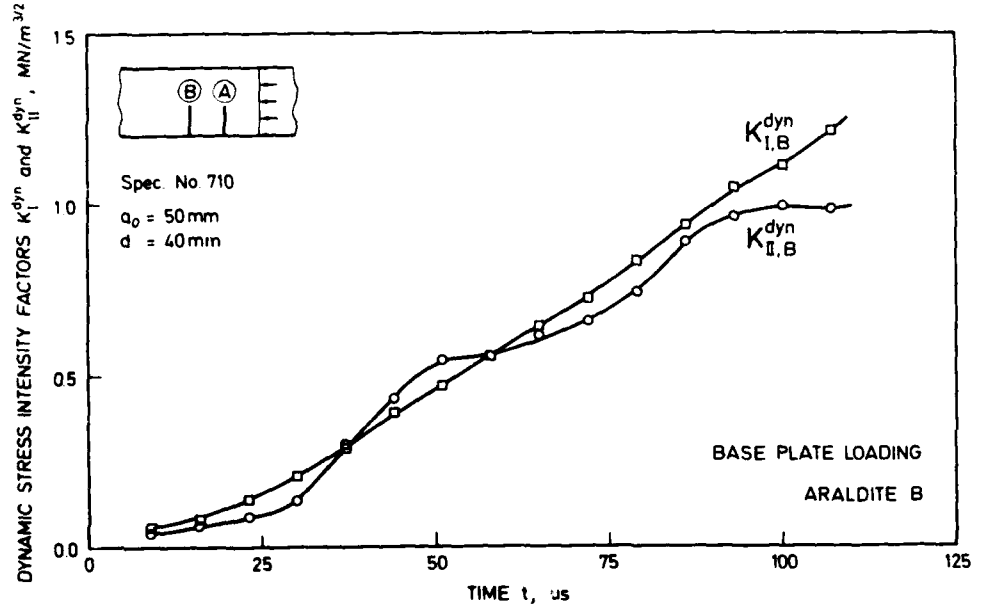

Fig. 29 Mode I and mode II stress intensity factors for a double crack configuration under base plate loading

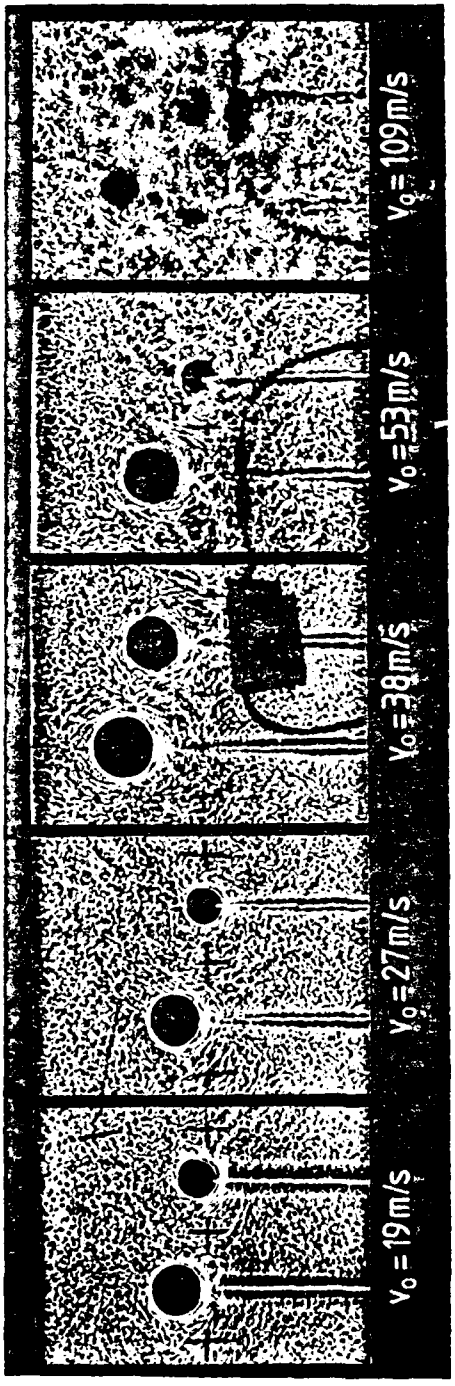

Fig. 30 Disturbance of caustics by air turbulence

are plottet as functions of time. As under direct loading conditions, the properties K_{Id}, t_f, and $\dot{K}_I^{dyn}$ can be obtained from these plots. Fig. 29 shows quantitative results for the right hand crack of the double crack configuration of Fig. 27. The stress intensity factor K_I^{dyn} and the mode-II stress intensity factor K_{II}^{dyn} are plotted as functions of time. Since the crack did not become unstable, the crack tip position is not shown. Data of this kind give information on the mutual interaction of multiple cracks under dynamic loading conditions.

Numerous experiments have been performed to study the reproducibility of the base plate loading arrangement. Early data indicate that the increase of the stress intensity factor with time was different although the impact conditions, in particular the impact velocities, where the same. More detailed investigations revealed a strong influence of the procedure how the specimens are fastened to the base plate. This difficulty was overcome by using fluted edges at the base plate and by fastening the specimens to the base plate in a controlled manner using a torque wrench.

A subsequent series of experiments has been performed by varying the impact velocity from about 10 m/s to 110 m/s. Fig. 30 shows the resulting shadow optical photographs. At higher impact velocities the pictures become disturbed by turbulances of the air following the projectile. Up to about 30 m/s this effect is of no influence. Up to 40 m/s the photographs can still be evaluated, but at higher velocities it is not possible anymore to derive reliable quantitative data. The base plate loading arrangement, therefore, is limited to a maximum impact velocity of about 40 m/s. The stress intensification rate then is of the order of 10^4 $MNm^{-3/2}s^{-1}$.

5 SUMMARY

Within the first year of the three year's research project the experimental set-up for investigating the fracture behavior under impact loading has been built up. The existing IWM gas gun has been modified for this purpose, a Cranz-Schardin camera operated in shadow optical arrangement has been aligned to the gas gun. A holding fixture has been designed and built to load the specimens under direct and base plate loading con ditions. The set-up has been successfully tested under different impact conditions, in particular the load pulse history in the specimen has been tested. Several series of experiments have been performed to specify the parameters for the following main investigations.

Thus the work is progressing according to schedule. The main experiments with a systematic variation of test parameters are planned to be carried out in the second year. These investigations will be performed predominantly with Araldite B specimens; for the third year investigations with high strength steel specimens are planned.

6 REFERENCES

[1] ASME Boiler and Pressure Vessel Code, The American Society of Mechanical Engineers, New York, N.Y., U.S.A.

[2] ASTM Book of Standards, Part 10, American Society for Testing and Materials, Philadelphia, Pa., U.S.A.

[3] ASTM E 24.03.03, "Proposed Standard Method of Tests for Instrumented Impact Testing of Precracked Charpy Specimens of Metallic Materials", Draft 2c, American Society for Testing and Materials, Philadelphia, U.S.A., 1980

[4] Kalthoff, J.F., Böhme, W., Winkler, S., and Klemm, W.: "Measurements of Dynamic Stress Intensity Factors in Impacted Bend Specimens", CSNI Specialist Meeting on Instrumented Precracked Charpy Testing, EPRI, Palo Alto, Calif., U.S.A., Dec. 1980

[5] Sih, G.C.: "Some Elastodynamic Problems of Cracks", Int. J. Fract. Mech. 4, 1968, 51-68

[6] Achenbach, J.D.: "Brittle and Ductile Extension of a Finite Crack by a Horizontally Polarized Shear Wave", Int. J. Engng. Sci. 8, 1970, 947-966

[7] Achenbach, J.D.: "Dynamic Effects in Brittle Fracture", Mechanics Today, Vol. 1, 1972, ed. by Nemat-Nasser, Pergamon

[8] Freund, L.B.: "Crack Propagation in an Elastic Solid Subjected to General Loading - III. Stress Wave Loading", J. Mech. Phys. Solids 21, 1973, 47-61

[9] Sih, G.C.: "Handbook of Stress Intensity Factors", Institute of Fracture and Solid Mechanics, 1973, Lehigh University, Bethlehem, Pa., U.S.A.

[10] Steverding, B., Lehnigk, S.H.: "Response of Cracks to Impact", J. Appl. Phys. 41, 1970, 2096-2099

[11] Steverding, B., Lehnigk, S.H.: "Collision of Stress Pulses with Obstacles and Dynamics of Fracture", J. Appl. Phys. 42, 1971, 3231-3238

[12] Lehnigk, S.H.: "A Macroscopic Dynamic Theory of Stability and Instability of Cracks Under Impulsive Loading", Dynamic Crack Propagation, ed. by G.C. Sih, Noordhoff-Groningen, 1973, 333

[13] Steverding, B.: "Fracture and Dislocation Dynamics", Dynamic Crack Propagation, ed. by G.C. Sih, Noordhoff-Groningen, 1973, 349

[14] Kalthoff, J.F., Shockey, D.A.: "On the Dynamic Instability of Cracks Loaded by Tensile Stress Pulses of Short Duration", Poulter Laboratory, Technical Report 001-75, 1974, Stanford Research Institute, Menlo Park, California

[15] Shockey, D.A., Kalthoff, J.F.: "Stability of Cracks Under High Rate Loads", Joint JSME-ASME Applied Mechanics Western Conf., 24-27 March 1975, Waikiki Beach, Honolulu, Hawai

[16] Kalthoff, J.F., Shockey, D.A.: "Instability of Cracks Under Impulse Loads", Journ. Appl. Phys. 48, 1977, 986-993

[17] Shockey, D.A., Kalthoff, J.F., and Ehrlich, D.C.: "Evaluation of Dynamic Crack Instability Criteria", to appear in Int. J. Fracture

[18] ASTM SPT 466 "Impact Testing of Metals", American Society for Testing and Materials, Philadelphia, Pa., 1974, U.S.A.

[19] ASTM STP 563 "Instrumented Impact Testing", American Society for Testing and Materials, Philadelphia, Pa., 1974, U.S.A.

[20] Shoemaker, A.K., Rolfe, S.T.: "The Static and Dynamic Low-Temperature Crack Toughness Performance of Seven Structural Steels", J. Engng. Fract. Mech., Vol. 2, 1971, 319-339

[21] Loss, J.F., Hawthorne, J.R., Griffis, C.A.: "Fracture Toughness of Light Water Reactor Pressure Vessel Materials", Naval Research Laboratory Memorandum Report 3036, 1975

[22] Proc. Int. Conf. Dynamic Fracture Toughness, London, July 5-7 1976

[23] Costin, L.S., Duffy, J., and Freund, L.B.: "Fracture Initiation in Metals Under Stress Wave Loading Conditions", ASTM STP 627, Fast Fract. and Crack Arrest, American Society for Testing and Materials. Philadelphia, Pa., U.S.A., 1977, 301

[24] Costin, L.S., Server, W.L., Duffy, J.: "Dynamic Fracture Initiation: A Comparison of Two Experimental Methods", to be published in ASME, J. of Engng. Materials and Technology

[25] Shockey, D.A., Curran, D.R.: "A Method for Measuring K_{Ic} at Very High Strain Rates", ASTM STP 536, American Society for Testing and Materials, Philadelphia, Pa., U.S.A., 1973, 297

[26] Homma, H., Shockey, D.A., and Muragama, Y.: "Respons[illegible] Cracks in Structural Materials to Short Pulse Loads", submitted to J. Mech. Phys. Solids

[27] Ravi Chandar, K., and Knauss, W.G.: "Dynamic Crack-Tip Stresses under Stress Wave Loading - A Comparison of Theory and Experiment" to appear in Int. Journ. of Fracture

[28] Eftis, J., Krafft, J.M.: "A Comparison of the Initiation with the Rapid Propagation of a Crack in a Mild Steel Plate", J. Basic Eng., 1965, 257

[29] Manogg, P.: "Anwendung der Schattenoptik zur Untersuchung des Zerreißvorgangs von Platten", Dissertation, Universität Freiburg, Germany, 1964

[30] Manogg, P.: "Schattenoptische Messung der spezifischen Bruchenergie während des Bruchvorgangs bei Plexiglas", Proceedings, International Conference on the Physics of Non-Crystalline Solids, Delft, The Netherlands, 1964, pp. 481-490

[31] Theocaris, P.S.: "Local Yielding Around a Crack Tip in Plexiglas", J. Appl. Mech., Vol. 37, 1970, pp. 409-415

[32] Beinert, J. and Kalthoff, J.F.: "Experimental Determination of Dynamic Stress Intensity Factors by Shadow Patterns" in Mechanics of Fracture, Vol. 7, Ed. G.C. Sih, Martinus Nijhoff Publishers, The Hague, Boston, London, 1981, pp. 281-330

[33] Kalthoff, J.F.: "Stress Intensity Factor Determination by Caustics", Intl. Conf. Experimental Mechanics, Society for Experimental Stress Analysis and Japan Society of Mechanical Engineers, Honolulu, Maui, Hawaii, U.S.A., May 23-28, 1982

[34] Kalthoff, J.F., Beinert, J., and Winkler, S.: "Measurements of Dynamic Stress Intensity Factors for Fast Running and Arresting Cracks in Double-Cantilever-Beam-Specimens", ASTM STP 627 - Fast Fracture and Crack Arrest, American Society for Testing and Materials, Philadelphia, U.S.A., 1977, pp. 161-176

[35] Kalthoff, J.F., Beinert, J., Winkler, S., and Klemm, W.: "Experimental Analysis of Dynamic Effects in Different Crack Arrest Test Specimens", ASTM STP 711 - Crack Arrest Methodology and Applications, American Society for Testing and Materials, Philadelphia, U.S.A., 1980, pp. 109-127

[36] Kalthoff, J.F., Beinert, J., Winkler, S.: "Analysis of Fast Running and Arresting Cracks by the Shadow Optical Method of Caustics", Symposium on Optical Methods of Mechanics of Solids, International Union of Theoretical and Applied Mechanics (IUTAM) Poitiers, France, Sept. 1979

[37] Kalthoff, J.F., Böhme, W., and Winkler, S.: "Analysis of Impact Fracture Phenomena by Means of the Shadow Optical Method of Caustics", VIIth Intl. Conf. Experimental Stress Analysis, Society for Experimental Stress Analysis, Haifa, Israel, Aug. 23-27, 1982

[38] Kalthoff, J.F., Winkler, S., Böhme, W. and Klemm, W.: "Determination of the Dynamic Fracture Toughness K_{Id} in Impact Tests by Means of Response Curves", 5th Intl. Conf. Fracture, Cannes, March 29 - April 3, 1981, Advances in Fracture Research, Ed. D. Francois et al., Pergamon Press, Oxford, New York, 1980

[39] Theocaris, P.S.: "Complex Stress-Intensity Factors at Bifurcated Cracks", J. Mech. Phys. Solids 20, 1972, 265-279

[40] Seidelmann, U.: "Anwendung des schattenoptischen Kaustikenverfahrens zur Bestimmung bruchmechanischer Kennwerte bei überlagerter Normal- und Scherbeanspruchung", IWM-Report 2/76, Fraunhofer-Institut für Werkstoffmechanik, Freiburg, 1976

[41] Beinert, J., Kalthoff, J.F., Seidelmann, U., and Soltész, U.: "Das schattenoptische Kaustikenverfahren und seine Anwendung in der Bruchmechanik", VDI-Berichte Nr. 207, pp. 15-25, VDI-Verlag, Düsseldorf, 1977

END

DATE
FILMED

1-84

DTIC